# UNIVERSIDAD DE CONCEPCIÓN

## Centro de Investigación en Ingeniería Matemática (CI²MA)

**A multilayer shallow water approach for polydisperse sedimentation with sediment compressibility and mixture viscosity**

Raimund Bürger, Enrique D. Fernández Nieto, Victor Osores

PREPRINT 2019-29

SERIE DE PRE-PUBLICACIONES

# A multilayer shallow water approach for polydisperse sedimentation with sediment compressibility and mixture viscosity

**Raimund Bürger · Enrique D. Fernández-Nieto · Víctor Osores**[1]

**Abstract** A three-dimensional multilayer shallow water approach to study polydisperse sedimentation and sediment transport in a viscous fluid is presented. The fluid is assumed be loaded with finely dispersed solid particles that belong to a finite number of species that differ in density and size. The model formulation allows one to recover the global mass and linear momentum balance laws of the mixture. The model incorporates compressibility of the sediment and viscosity of the mixture through a viscous stress tensor. As a consequence of a dimensional analysis applied to the global mass conservation and linear momentum balance equations, the horizontal components of the compression term and the horizontal terms of the viscous stress tensor may be neglected. This results in a final model that is vertically consistent with the classical one-dimensional vertical model. Numerical simulations illustrate the coupled solids volume fraction and flow fields in various scenarios and the effect of the compressibility and viscosity terms. Various bottom topographies give rise to recirculation of the fluid and high solids volume fractions on the bottom.

**Keywords**: multilayer shallow water model, polydisperse sedimentation, nonconservative products, path-conservative method, sediment compressibility, viscosity mixture, recirculation.

**Mathematics Subject Classifications**: 65N06, 76T20.

---

Raimund Bürger
CI$^2$MA and Departamento de Ingeniería Matemática, Facultad de Ciencias Físicas y Matemáticas, Universidad de Concepción, Casilla 160-C, Concepción, Chile.
E-mail: rburger@ing-mat.udec.cl

Enrique D. Fernández-Nieto
Departamento de Matemática Aplicada I, ETS Arquitectura, Universidad de Sevilla, Avda. Reina Mercedes No. 2, E-41012 Sevilla, Spain.
E-mail: edofer@us.es

Víctor Osores, [1]Corresponding author
CI$^2$MA and Departamento de Ingeniería Matemática, Facultad de Ciencias Físicas y Matemáticas, Universidad de Concepción, Casilla 160-C, Concepción, Chile.
E-mail: victorosores@udec.cl

# 1 Introduction

## 1.1 Scope

Mathematical models for the sedimentation of small particles suspended in a viscous fluid combined with the flow of the solid-fluid mixture are important to describe geophysical processes such as settling and sediment transport in rivers and estuaries as well as industrial applications in mineral processing, wastewater treatment, and other fields. [3,5,15,20,23]. It is frequently assumed that the volume fractions (concentrations) of the solid species are constant in each horizontal cross section, wall effects are neglected, and all field variables are assumed to depend on the vertical coordinate and time only. These assumptions lead to a one-dimensional vertical model that is aligned with the gravity body force [8–10], which is adequate for models of unit operations in industrial applications. In this work we are interested in modeling polydisperse sedimentation processes that not only depend on the vertical direction (in which segregation of the species take place), but that are subject to a significant horizontal bulk flow in two horizontal directions.

In [11] we introduced a multilayer shallow water model for polydisperse sedimentation without viscous stress tensor and sediment compressibility. The goal is here to introduce these terms and to solve the resulting model numerically. In [13,21] the authors included terms accounting for sediment compressibility to one-dimensional sedimentation models. A theory of polydisperse sedimentation with compressibility terms was developed in [4] for a three-dimensional setting, but numerical results were presented for one space dimension only. Efficient implicit-explicit (IMEX) numerical techniques to solve the one-dimensional sedimentation model with compressibility terms and related strongly degenerate parabolic-hyperbolic equations are presented in [6, 7, 12].

Multilayer models are designed to avoid solving a fully three-dimensional model (such as the three-dimensional Navier-Stokes equations for an incompressible fluid) and are based on the so-called shallow water or Saint-Venant approach, that is, a vertically integrated version of the underlying model [1, 2, 24]. The multilayer approach consists in subdividing the computational domain into $M$ layers in the vertical direction, which leads to a system of Saint-Venant equations. Typically, under some hypothesis the unknowns are horizontal velocities by layer, the total height of the fluid column, and the solids concentrations for each species in each layer and in some cases as in [11] the total mass of the mixture. The vertical velocity of the mixture in each layer can be calculated by post-processing data, and we do not need to solve a partial differential equations to obtain this quantity.

It is the purpose of this paper to develop a multilayer shallow water model for three-dimensional polydisperse sedimentation process with the property that is possible to recover the mass and linear momentum balance laws of the mixture, which means that the mixture description is consistent with a single-phase flow model. Furthermore, and in contrast to previous efforts [11,17], sediment compressibility and viscosity of the mixture are talen into account. As in [11] we use a mass-average velocity and definition for total density of the mixture such that is possible to recover global mass and linear momentum balance of the mixture. The novelty of the present work, besides the introduction of the compressibility and mixture viscosity terms and their numerical treatment, is the use of a rotational invariance property of the equations to design the numerical method.

### 1.2 Outline of the paper

The paper is organized as follows. In Section 2 we introduce the partial differential equations (PDEs) governing polydisperse sedimentation coupled with the multilayer shallow water approach, introducing the continuity and the linear momentum balances equations for the solids, fluid phases and for the mixture in Section 2.1. In Section 2.2 we define the solid-fluid relative velocity for each solid phase. These velocities include the effective solid stress and the modified form of the Masliyah-Lockett-Bassoon (MLB; [18, 19]) model introduced in [11]. The effective solid stress is only active during consolidation, that is wherever the local total solids volume fraction $\phi$ exceeds a critical concentration or gel point $\phi_{\mathrm{c}}$. The final form of the multilayer approach with sediment compressibility and mixture viscosity is summarized in Section 2.3. A dimensional analysis is applied to mass and linear momentum balance equations in Section 3 in order to attain a simplified system of governing PDEs. The notation used in [11], and which is also employed here, for layers, interfaces, and boundaries of the multilayer approach is summarized in Sections 4.1 and 4.2. The notion of a weak solution to the governing multilayer PDEs, based on appropriate jump conditions across the each interface between adjacent layers, is introduced in Section 4.3. Mass and linear momentum jump conditions across the interlayer interfaces and the approximation of viscous stress tensors at the interfaces are computed in Section 4.4. To finish this section, in Section 4.5 we recover vertical velocities of the mixture in each layer by post-processing of data. The multilayer model that will eventually be solved is derived in Section 5. To this end we introduce in Section 5.1 the assumption of a hydrostatic pressure. Then we recall that the multilayer approach arises from a variational formulation of the balance equations, and notice that the multilayer model is a particular weak solution of these variational identities. The corresponding weak formulation in introduced in Section 5.2. Then, in Section 5.3 we use the dimensional analysis done in Section 3 to compute the final form of the multilayer model (returning to the original variables). Finally, the model is closed in Section 5.4 by establishing that the thickness of each layer is a fixed fraction of the total height of the fluid, and the final form of the equations that will actually be solved is developed. In Section 6 we formulate a 2D numerical scheme to solve this model. using the rotational invariance property of the system to solve and simulate polydisperse sedimentation process over different scenarios. Finally in Section 7 we present four numerical examples and some impression of the results. First, in Section 7.1 we simulate a bi-bidisperse sedimentation process in two horizontal space dimension over a domain with a bump (Test 1), where the compressibility of the sediment and viscosity mixture terms are deactivated, this simulation is the 3D version of (Test 3) in [11]. In Section 7.2 we simulate a cylindrical dam break bidisperse sedimentation process over paraboloid bottom and we compare the behavior of the mixture where the sediment compressibility and mixture viscosity terms are activated and deactivated respectively. In Section 7.3 we simulate a bidisperse sedimentation over a real bathymetry, compression and mixture viscosity terms activated, here we compare the behavior of the mixture for various values of the gel point $\phi_{\mathrm{c}}$. Finally in Section 7.4 we simulate the same mixture before but we have simulated for different $\sigma_0$ keeping constant the gel point at $\phi_{\mathrm{c}} = 0.1$. Some conclusions are collected in Section 8.

## 2 Governing equations

### 2.1 Continuity equations and linear momentum balances

Let us consider $N \in \mathbb{N}$ species of spherical solid particles dispersed in a viscous fluid. For each solid species $j$, $j = 1, \dots, N$, we denote by $\phi_j$, $\rho_j$, and $d_j$ its volumetric concentration, density, and particle diameter, respectively. Furthermore, we denote by $\boldsymbol{v}_j = (u_j, v_j, w_j)^{\mathrm{T}} \in \mathbb{R}^3$ its phase velocity with the horizontal component $(u_j, v_j) \in \mathbb{R}^2$ and vertical component $w_j \in \mathbb{R}$. The same notation is used for the fluid indexed by $j = 0$. The model is based on the continuity and linear momentum balance equations for the $N$ solid species and the fluid. As in [11], for $j = 0, \dots, N$ the continuity and linear momentum equations are given by

$$
\begin{aligned}
&\partial_t(\rho_j\phi_j) + \nabla \cdot (\rho_j\phi_j\boldsymbol{v}_j) = 0,\\
&\partial_t(\rho_j\phi_j\boldsymbol{v}_j) + \nabla \cdot (\rho_j\phi_j\boldsymbol{v}_j \otimes \boldsymbol{v}_j) = \nabla \cdot \boldsymbol{T}_j + \rho_j\phi_j\boldsymbol{b} + \boldsymbol{m}_j^{\mathrm{f}} + \boldsymbol{m}_j^{\mathrm{s}}, \quad j = 0, \dots, N,
\end{aligned}
\tag{2.1}
$$

where $\boldsymbol{T}_j$ denotes the stress tensor of particle species $j$, $j = 1, \dots, N$, $\boldsymbol{T}_0$ that of the fluid, $\boldsymbol{b}$ is the body force, $\boldsymbol{m}_j^{\mathrm{f}}$ and $\boldsymbol{m}_{ji}^{\mathrm{s}}$ are the interaction forces per unit volume between solid species $j$ and the fluid and between the solid species $j$ and $i$, respectively, and $\boldsymbol{m}_j^{\mathrm{s}} = \boldsymbol{m}_{j1}^{\mathrm{s}} + \dots + \boldsymbol{m}_{jN}^{\mathrm{s}}$ is the particle-particle interaction terms of species $j$. For the fluid we obtain $\boldsymbol{m}_0^{\mathrm{f}} = -\boldsymbol{m}_1^{\mathrm{f}} - \dots - \boldsymbol{m}_N^{\mathrm{f}}$ and $\boldsymbol{m}_0^{\mathrm{s}} = 0$. For very low Reynolds numbers there is considerable experimental and theoretical justification [4] for neglecting the quantities $\boldsymbol{m}_{ji}^{\mathrm{s}}$. Let $\Phi := (\phi_0, \dots, \phi_N)^{\mathrm{T}}$. We define the density $\rho = \rho(\Phi)$ of the mixture and its mass-average velocity $\boldsymbol{v}$ by

$$
\begin{aligned}
&\rho := \rho(\Phi) := \rho_0\phi_0 + \rho_1\phi_1 + \dots + \rho_N\phi_N,\\
&\boldsymbol{v} := (u, v, w)^{\mathrm{T}} := \frac{1}{\rho}\sum_{m=0}^{N} \rho_m\phi_m\boldsymbol{v}_m = \frac{1}{\rho}\left[\left(\rho - \sum_{j=1}^{N}\rho_j\phi_j\right)\boldsymbol{v}_0 + \sum_{k=1}^{N}\rho_k\phi_k\boldsymbol{v}_k\right],
\end{aligned}
\tag{2.2}
$$

The importance of defining the average velocity $\boldsymbol{v}$ precisely as is done in (2.2) is that this formulation allows us to recover the global mass and linear momentum balance laws for the mixture. In fact, summing from $j = 0$ to $j = N$ the continuity and linear momentum balance equations (2.1) yields

$$
\partial_t\rho + \nabla \cdot (\rho\boldsymbol{v}) = 0, \quad \partial_t(\rho\boldsymbol{v}) + \nabla \cdot (\rho\boldsymbol{v} \otimes \boldsymbol{v}) = \nabla \cdot \boldsymbol{\Sigma} + \rho\boldsymbol{b}, \tag{2.3}
$$

where $\rho$ and $\boldsymbol{v}$ are given by (2.2) and setting $\boldsymbol{T} := \boldsymbol{T}_0 + \boldsymbol{T}_1 + \dots + \boldsymbol{T}_N$ and defining the diffusion velocities $\boldsymbol{u}_j^{\mathrm{d}} := \boldsymbol{v}_j - \boldsymbol{v}$, the stress tensor of the mixture

$$
\boldsymbol{\Sigma} := \boldsymbol{T} - \sum_{j=0}^{N}\rho_j\phi_j\boldsymbol{u}_j^{\mathrm{d}} \otimes \boldsymbol{u}_j^{\mathrm{d}}
$$

is obtained. The stress tensor of each solid phase can be written as $\boldsymbol{T}_j = -p_j\boldsymbol{I} + \boldsymbol{T}_j^{\mathrm{E}}$, where $p_j = (\phi_j/\phi)(\phi p + \sigma_{\mathrm{e}}(\phi))$ is the pressure of phase $j$ for $j = 1, \dots, N$. For the stress tensor of the fluid we get $p_0 = (1-\phi)p$. The total concentration of particles is $\phi = \phi_1 + \dots + \phi_N$ and $\boldsymbol{T}_0^{\mathrm{E}}$ and $\boldsymbol{T}_j^{\mathrm{E}}$ are viscous stress tensors of the fluid and solid phases, respectively. The effective solid stress $\sigma_{\mathrm{e}}(\phi)$ can be defined by

$$
\sigma_{\mathrm{e}}(\phi) = \begin{cases} 0 & \text{for } \phi \le \phi_{\mathrm{c}},\\ \sigma_0\left((\phi/\phi_{\mathrm{c}})^k - 1\right) & \text{for } \phi > \phi_{\mathrm{c}}, \end{cases} \qquad \sigma_{\mathrm{e}}'(\phi) = \begin{cases} 0 & \text{for } \phi \le \phi_{\mathrm{c}},\\ (\sigma_0/\phi_{\mathrm{c}}^k)k\phi^{k-1} & \text{for } \phi > \phi_{\mathrm{c}} \end{cases} \tag{2.4}
$$

with parameters $\sigma_0 > 0$ and $k \ge 1$, and where $\phi_{\mathrm{c}}$ denotes the so-called critical concentration or gel point. Values for real materials for these parameters can be found in the literature. The solid-fluid interaction force per unit volume is given by $\boldsymbol{m}_j^{\mathrm{f}} = \alpha_j(\Phi)\boldsymbol{u}_j + p\nabla\phi_j$, where $\alpha_j$ is the resistance coefficient for the transfer of momentum between the fluid and solid phase species $j$ [4]. Finally here we assume that gravity is the only body force, i.e., $\boldsymbol{b} = g\boldsymbol{k}$, where $\boldsymbol{k}$ is the downward-pointing unit vector.

Defining the slip velocities $\boldsymbol{u}_j := \boldsymbol{v}_j - \boldsymbol{v}_0$ (including $\boldsymbol{u}_0 = \boldsymbol{0}$) and $\lambda_j := \rho_j\phi_j/\rho$ for $j = 1,\dots,N$, we can derive for each solid species

$$\rho_j\phi_j\boldsymbol{v}_j = \rho_j\phi_j\big(\boldsymbol{u}_j + \boldsymbol{v} - (\lambda_1\boldsymbol{u}_1 + \dots + \lambda_N\boldsymbol{u}_N)\big), \quad j = 0,\dots,N; \tag{2.5}$$

hence as in [11] the mass and linear momentum equations for all phases are given by

$$\begin{aligned}
&\partial_t(\rho_j\phi_j) + \nabla\cdot\big(\rho_j\phi_j\big(\boldsymbol{u}_j + \boldsymbol{v} - (\lambda_1\boldsymbol{u}_1 + \dots + \lambda_N\boldsymbol{u}_N)\big)\big) = 0, \quad j = 0,\dots N,\\
&\rho_j\phi_j\mathrm{D}_t\boldsymbol{v}_j = \nabla\cdot\boldsymbol{T}_j^{\mathrm{E}} - \phi_j\nabla p - \rho_j\phi_j g\boldsymbol{k} + \alpha_j\boldsymbol{u}_j - \nabla\left(\frac{\phi_j}{\phi}\sigma_{\mathrm{e}}(\phi)\right), \quad j = 1,\dots,N,\\
&\rho_0(1-\phi)D_t\boldsymbol{v}_0 = -(1-\phi)\nabla p + \nabla\cdot\boldsymbol{T}_0^{\mathrm{E}} + \rho_0(1-\phi)g\boldsymbol{k} - (\alpha_1\boldsymbol{u}_1 + \dots + \alpha_N\boldsymbol{u}_N),
\end{aligned} \tag{2.6}$$

where we have used the standard notation $\mathrm{D}_t\boldsymbol{v} = \partial_t\boldsymbol{v} + (\boldsymbol{v}\cdot\nabla)\boldsymbol{v}$. The systems of equationss (2.1) and (2.6) are equivalent and therefore both allow us to recover (2.3).

## 2.2 Explicit formula for the slip velocities $\boldsymbol{u}_j$

The system (2.6) is closed by an explicit expression for the slip velocities $\boldsymbol{u}_j$. In [4] the explicit formula

$$\boldsymbol{u}_j = g\frac{\phi_j}{\alpha_j(\Phi)}\left((\bar\rho_j - \bar{\boldsymbol{\rho}}^{\mathrm{T}}\Phi)\boldsymbol{k} + \frac{\sigma_{\mathrm{e}}(\phi)}{g\phi_j}\nabla\left(\frac{\phi_j}{\phi}\right) + \frac{1-\phi}{g\phi}\nabla\sigma_{\mathrm{e}}(\phi)\right), \quad j = 1,\dots,N. \tag{2.7}$$

for these relative velocities was derived, where $\bar\rho_j := \rho_j - \rho_0$ for $j = 1,\dots,N$ are reduced densities and $\bar{\boldsymbol{\rho}} := (\bar\rho_1,\dots,\bar\rho_N)^{\mathrm{T}}$. In [11] we only considered the case when $\sigma_{\mathrm{e}} \equiv 0$, that is, sediment compressibility was not taken into account. In other words, the slip velocities used in [11] are the simplest possible, namely

$$\boldsymbol{u}_j = g\frac{\phi_j}{\alpha_j(\Phi)}(\bar\rho_j - \bar{\boldsymbol{\rho}}^{\mathrm{T}}\Phi)\boldsymbol{k}, \quad j = 1,\dots,N.$$

Following [4, 11, 18, 19] we choose $\phi_j/\alpha_j(\Phi) = -d_j^2V(\phi)/18\mu_0$, where $\mu_0$ is the viscosity of the pure fluid, and $V(\phi)$ is a hindrance factor that is assumed to satisfy $V(\phi) > 0$ and $V'(\phi) < 0$ for $0 < \phi < \phi_{\max}$. This factor can be chosen as the Richardson-Zaki [22] function

$$V(\phi) = \begin{cases}(1-\phi)^{n_{\mathrm{RZ}}-2} & \text{for } \phi \le \phi_{\max},\\ 0 & \text{for } \phi > \phi_{\max},\end{cases} \quad n_{\mathrm{RZ}} > 2. \tag{2.8}$$

Setting $\mu := -gd_1^2/(18\mu_0)$ and $\delta_j := d_j^2/d_1^2$, $j = 1,\dots,N$, we obtain the final form of the slip velocities

$$\boldsymbol{u}_j = \mu\delta_jV(\phi)\left((\bar\rho_j - \bar{\boldsymbol{\rho}}^{\mathrm{T}}\Phi)\boldsymbol{k} + \frac{\sigma_{\mathrm{e}}(\phi)}{g\phi_j}\nabla\left(\frac{\phi_j}{\phi}\right) + \frac{1-\phi}{g\phi}\nabla\sigma_{\mathrm{e}}(\phi)\right), \quad j = 1,\dots,N. \tag{2.9}$$

Inserting (2.9) into (2.5) and denoting $\Phi := (\phi_1,\dots,\phi_N)^{\mathrm{T}}$ and let $\boldsymbol{\delta} := (\delta_1,\dots,\delta_N)^{\mathrm{T}}$, $\boldsymbol{\lambda} := (\lambda_1,\dots,\lambda_N)^{\mathrm{T}}$ we get that for each solid species $\rho_j\phi_j\boldsymbol{v}_j = \rho_jf_j^{\mathrm{M}}(\Phi)\boldsymbol{k} + \rho_j\phi_j\boldsymbol{v} - \boldsymbol{a}_j(\Phi,\nabla\Phi)$, where we define for $j = 1,\dots,N$

$$\begin{aligned}
f_j^{\mathrm{M}}(\Phi) &:= \phi_jv_j^{\mathrm{MLB}} = \phi_j\mu V(\phi)\left(\delta_j(\bar\rho_j - \bar{\boldsymbol{\rho}}^{\mathrm{T}}\Phi) - \sum_{k=1}^N\lambda_k\delta_k(\bar\rho_k - \bar{\boldsymbol{\rho}}^{\mathrm{T}}\Phi)\right),\\
\boldsymbol{a}_j(\Phi,\nabla\Phi) &:= -\frac{\mu}{g}\rho_jV(\phi)\left\{\frac{(1-\phi)\phi_j}{\phi}(\delta_j - \boldsymbol{\delta}^{\mathrm{T}}\boldsymbol{\lambda})\nabla\sigma_{\mathrm{e}}(\phi) + \sigma_{\mathrm{e}}(\phi)\left[\delta_j\nabla\left(\frac{\phi_j}{\phi}\right) - \phi_j\sum_{i=1}^N\frac{\lambda_i\delta_i}{\phi_i}\nabla\left(\frac{\phi_i}{\phi}\right)\right]\right\}.
\end{aligned}$$

Consistently with the global mass conservation (2.1), we define $f_0^{\mathrm{M}} := (\rho_1 f_1^{\mathrm{M}} + \cdots + \rho_N f_N^{\mathrm{M}})/\rho_0$ and $\boldsymbol{a}_0 := -(\boldsymbol{a}_1 + \cdots + \boldsymbol{a}_N)$.

Note that the velocity of each phase is much more complicated than in the framework of [11]. This new approach poses extreme difficulties for the attempt to solve (2.1). Without going into detail, we do no longer have the property that the horizontal velocity of each species equals that of the mixture. This difficulty will be handled in Section 3.

*Remark 1* If $\phi \leq \phi_{\mathrm{c}}$, then the horizontal velocity of each species equals that of the mixture and only the vertical velocity of each species differs from that of the mixture, as can be inferred from

$$\rho_j \phi_j w_j = \rho_j \phi_j w + \rho_j f_j^{\mathrm{M}}(\Phi).$$

### 2.3 Final form of the model equations

The final model is given by the mass and linear momentum balance equations for each species plus the fluid after substituting (2.7) into (2.6). It can be written as

$$\partial_t(\rho_j \phi_j) + \nabla \cdot (\rho_j \phi_j \boldsymbol{v} + \rho_j f_j^{\mathrm{M}}(\Phi)\boldsymbol{k}) = \nabla \cdot \boldsymbol{a}_j(\Phi, \nabla \Phi), \quad j = 0, \dots, N, \tag{2.10}$$

$$\rho_j \phi_j \mathrm{D}_t \boldsymbol{v}_j = \nabla \cdot \boldsymbol{T}_j^{\mathrm{E}} - \phi_j \nabla p - \phi_j \rho g \boldsymbol{k} - \phi_j \nabla \sigma_{\mathrm{e}}(\phi), \quad j = 0, \dots, N. \tag{2.11}$$

Summing up from $j = 0$ to $j = N$ the linear momentum balance equations (2.6) yields

$$\partial_t \left( \sum_{j=0}^{N} \rho_j \phi_j \boldsymbol{v}_j \right) + \nabla \cdot \left( \sum_{j=0}^{N} \rho_j \phi_j \boldsymbol{v}_j \otimes \boldsymbol{v}_j \right) = \nabla \cdot \boldsymbol{T} - \rho g \boldsymbol{k}, \tag{2.12}$$

where $\boldsymbol{T} = \sum_{j=0}^{N} \boldsymbol{T}_j = -(p + \sigma_{\mathrm{e}}(\phi))\boldsymbol{I} + \boldsymbol{T}^{\mathrm{E}}$, where $p$ is pressure and the extra stress tensor $\boldsymbol{T}^{\mathrm{E}}$ is given by $\boldsymbol{T}^{\mathrm{E}} = \frac{\eta}{2}\boldsymbol{D}(\boldsymbol{v}) + \lambda \nabla \cdot (\boldsymbol{v})\boldsymbol{I}$, where $\eta, \lambda \geq 0$ are viscosity terms. The strain rate $\boldsymbol{D}(\boldsymbol{v})$ tensor is given by $\boldsymbol{D}(\boldsymbol{v}) = \nabla \boldsymbol{v} + (\nabla \boldsymbol{v})^{\mathrm{T}}$.

## 3 Dimensional analysis

By a dimensional analysis we now show that only terms in the vertical direction of the extra stress tensor are important. Others terms will be discarded under the assumptions of a shallow domain, that is, the characteristic height ($H$) will be assumed smaller than the characteristic length ($L$). In other words, we assume that $\varepsilon := H/L$ is small.

We define the following dimensionless variables: $(x, y, z) = (L\tilde{x}, L\tilde{y}, H\tilde{z})$ for spatial position and $t = (L/U)\tilde{t}$ for the characteristic time. The relation between the spatial gradient $\nabla$ and the dimensionless gradient $\tilde{\nabla}$ is defined by $\nabla = (1/L)\boldsymbol{I}_\varepsilon \tilde{\nabla}$, where $\boldsymbol{I}_\varepsilon := \mathrm{diag}(1, 1, 1/\varepsilon)$. The dimensionless time derivative is $\partial/\partial t = (U/L)\partial/\partial \tilde{t}$. We use in some cases the following definitions for the velocity vector to simplify notatation: $\boldsymbol{v}_\varepsilon := (\tilde{u}, \tilde{v}, \varepsilon \tilde{w})$, $\boldsymbol{v}_{\varepsilon,j} := (\tilde{u}_j, \tilde{v}_j, \varepsilon \tilde{w}_j)$, $\tilde{\boldsymbol{v}} := (\tilde{u}, \tilde{v}, \tilde{w})$, and $\tilde{\boldsymbol{v}}_j = (\tilde{u}_j, \tilde{v}_j, \tilde{w}_j)$. Furthermore, for height, densities, pressure, and viscosities we have $h = H\tilde{h}$, $\rho_j = \bar{\rho}_0 \tilde{\rho}_j$, $P = \bar{\rho}_0 U^2 \tilde{P}$, $\sigma_{\mathrm{e}} = \bar{\rho}_0 U^2 \tilde{\sigma}_e$, $\eta = \bar{\rho}_0 U H \tilde{\eta}$, $\lambda = \bar{\rho}_0 U H \tilde{\lambda}$, $\mu_0 = \bar{\rho}_0 U H \tilde{\mu}_0$, $d_1 = H\tilde{d}_1$, and $\mu/g = H\tilde{d}_1/(18\bar{\rho}_0 U \tilde{\mu}_0)$. From here so on dimensionless variables will be denoted with the tilde symbol ($\tilde{\ }$). In light of $\boldsymbol{v}_j = (u_j, v_j, w_j) = U\boldsymbol{v}_{\varepsilon,j}$, the mass average velocity $\boldsymbol{v}$ of the mixture satisfies

$$\boldsymbol{v} = \sum_{j=0}^{N} \frac{\rho_j \phi_j}{\rho}(u_j, v_j, w_j) = U \sum_{j=0}^{N} \frac{\tilde{\rho}_j \phi_j}{\tilde{\rho}}(\tilde{u}_j, \tilde{v}_j, \varepsilon \tilde{w}_j) = U \sum_{j=0}^{N} \frac{\tilde{\rho}_j \phi_j}{\tilde{\rho}} \boldsymbol{v}_{\varepsilon,j} = U \boldsymbol{v}_\varepsilon,$$

Furthermore, the equalities $\rho_j\phi_j\boldsymbol{v}_j = \bar\rho_0 U\tilde\rho_j\phi_j\boldsymbol{v}_{\varepsilon,j}$ and

$$\rho_j f_j^{\mathrm{M}}(\Phi)\boldsymbol{k} + \rho_j\phi_j\boldsymbol{v} - \boldsymbol{a}_j(\Phi,\nabla\Phi) = \bar\rho_0 U\big(\tilde\rho_j\tilde f_j^{\mathrm{M}}(\Phi)\boldsymbol{k} + \tilde\rho_j\phi_j\boldsymbol{v}_\varepsilon - \varepsilon\boldsymbol{I}_\varepsilon\tilde{\boldsymbol{a}}_j(\Phi,\nabla\Phi)\big)$$

imply that

$$\bar\rho_0 U\tilde\rho_j\phi_j\boldsymbol{v}_{\varepsilon,j} = \bar\rho_0 U\big(\tilde\rho_j\tilde f_j^{\mathrm{M}}(\Phi)\boldsymbol{k} + \tilde\rho_j\phi_j\boldsymbol{v}_\varepsilon - \varepsilon\boldsymbol{I}_\varepsilon\tilde{\boldsymbol{a}}_j(\Phi,\nabla\Phi)\big). \tag{3.1}$$

In light of the previous equalities, the mass balance of each solid species (2.10) can be written as

$$\frac{\bar\rho_0 U}{L}\partial_{\tilde t}(\tilde\rho_j\phi_j) + \frac{\bar\rho_0 U}{L}\tilde\nabla\cdot\big(\boldsymbol{I}_\varepsilon(\tilde\rho_j\phi_j\boldsymbol{v}_\varepsilon + \tilde\rho_j\tilde f_j^M(\Phi)\boldsymbol{k})\big) = \frac{\bar\rho_0 U}{L}\tilde\nabla\cdot(\varepsilon\boldsymbol{I}_\varepsilon^2\tilde{\boldsymbol{a}}_j), \tag{3.2}$$

then we get the dimensionless partial differential equation for the mass balance of each species

$$\partial_{\tilde t}(\tilde\rho_j\phi_j) + \tilde\nabla\cdot\left(\tilde\rho_j\phi_j\tilde{\boldsymbol{v}} + \frac{1}{\varepsilon}\tilde\rho_j\tilde f_j^M(\Phi)\boldsymbol{k}\right) = \tilde\nabla\cdot(\varepsilon\boldsymbol{I}_\varepsilon^2\tilde{\boldsymbol{a}}_j), \tag{3.3}$$

or equivalently, applying the matrix $\boldsymbol{I}_\varepsilon$ to equality (3.1),

$$\partial_{\tilde t}(\tilde\rho_j\phi_j) + \tilde\nabla\cdot(\tilde\rho_j\phi_j\tilde{\boldsymbol{v}}_j) = 0. \tag{3.4}$$

Furthermore, we define the dimensionless horizontal component of the strain-rate

$$\boldsymbol{D}_{\varepsilon,\mathrm{h}}(\tilde{\boldsymbol{v}}) := \tilde\nabla_{\tilde{\boldsymbol{x}}}\tilde{\boldsymbol{v}}_{\mathrm{h}} + (\tilde\nabla_{\tilde{\boldsymbol{x}}}\tilde{\boldsymbol{v}}_{\mathrm{h}})^{\mathrm{T}},$$

notice that $\rho_j\phi_j\boldsymbol{v}_j\otimes\boldsymbol{v}_j = \bar\rho_0 U^2\tilde\rho_j\phi_j\boldsymbol{v}_{\varepsilon,j}\otimes\boldsymbol{v}_{\varepsilon,j}$, and rewrite the total pressure $p_{\mathrm{tot}} := p + \sigma_{\mathrm{e}}(\phi)$ as $p_{\mathrm{tot}} = \bar\rho_0 U^2(\tilde p + \tilde\sigma_{\mathrm{e}}(\phi)) =: \bar\rho_0 U^2\tilde p_{\mathrm{tot}}$. and $\rho g\boldsymbol{k} = \bar\rho_0 U^2\tilde\rho/(\varepsilon\mathrm{Fr}^2 L)\boldsymbol{k}$, where the Froude number is given by $\mathrm{Fr} = \sqrt{gH}$, so we get

$$\begin{aligned}&\frac{\bar\rho_0 U^2}{L}\partial_{\tilde t}\left(\sum_{j=0}^N\tilde\rho_j\phi_j\boldsymbol{v}_{\varepsilon,j}\right) + \frac{\bar\rho_0 U^2}{L}\tilde\nabla\cdot\left(\sum_{j=0}^N\tilde\rho_j\phi_j\boldsymbol{v}_{\varepsilon,j}\otimes(\boldsymbol{I}_\varepsilon\boldsymbol{v}_{\varepsilon,j})\right)\\ &= \frac{\bar\rho_0 U^2}{L}\tilde\nabla\cdot\big(\tilde p_{\mathrm{tot}}\boldsymbol{I} + \tilde{\boldsymbol{T}}_\varepsilon^{\mathrm{E}}(\tilde{\boldsymbol{v}})\big)\boldsymbol{I}_\varepsilon - \frac{\bar\rho_0 U^2\tilde\rho}{L\mathrm{Fr}^2\varepsilon}\boldsymbol{k},\end{aligned} \tag{3.5}$$

where $\tilde{\boldsymbol{T}}_\varepsilon^{\mathrm{E}}$ is a dimensionless viscous stress tensor. Finally setting $\tilde{\boldsymbol{I}} = \varepsilon\boldsymbol{I}_\varepsilon$, we may rewrite the dimensionless linear momentum balance equation (3.5) as

$$\partial_{\tilde t}\left(\sum_{j=0}^N\tilde\rho_j\phi_j\boldsymbol{v}_{\varepsilon,j}\right) + \tilde\nabla\cdot\left(\sum_{j=0}^N\tilde\rho_j\phi_j\boldsymbol{v}_{\varepsilon,j}\otimes\boldsymbol{v}_j\right) = \frac{1}{\varepsilon}\tilde\nabla\cdot(\boldsymbol{\Sigma}\tilde{\boldsymbol{I}}) - \frac{1}{\varepsilon}\frac{\tilde\rho}{\mathrm{Fr}^2}\boldsymbol{k}, \tag{3.6}$$

where the dimensionless stress tensor is $\boldsymbol{\Sigma} := \tilde p_{\mathrm{tot}}\boldsymbol{I} + \tilde{\boldsymbol{T}}_\varepsilon^{\mathrm{E}}(\tilde{\boldsymbol{v}})$ with the dimensionless viscous stress tensor

$$\tilde{\boldsymbol{T}}_\varepsilon^{\mathrm{E}}(\tilde{\boldsymbol{v}}) = \frac{\tilde\eta}{2}\boldsymbol{D}_\varepsilon(\tilde{\boldsymbol{v}}) + 2\varepsilon\tilde\lambda(\tilde\nabla\cdot\tilde{\boldsymbol{v}})\boldsymbol{I},$$

where

$$\boldsymbol{D}_\varepsilon(\tilde{\boldsymbol{v}}) := \begin{bmatrix}\varepsilon\boldsymbol{D}_{\varepsilon,\mathrm{h}}(\tilde{\boldsymbol{v}}) & \partial_{\tilde z}\tilde{\boldsymbol{v}}_{\mathrm{h}} + \varepsilon^2(\tilde\nabla_x\tilde w)^{\mathrm{T}}\\ (\partial_{\tilde z}\tilde{\boldsymbol{v}}_{\mathrm{h}})^{\mathrm{T}} + \varepsilon^2\tilde\nabla_x\tilde w & 2\varepsilon\partial_{\tilde z}\tilde w\end{bmatrix}. \tag{3.7}$$

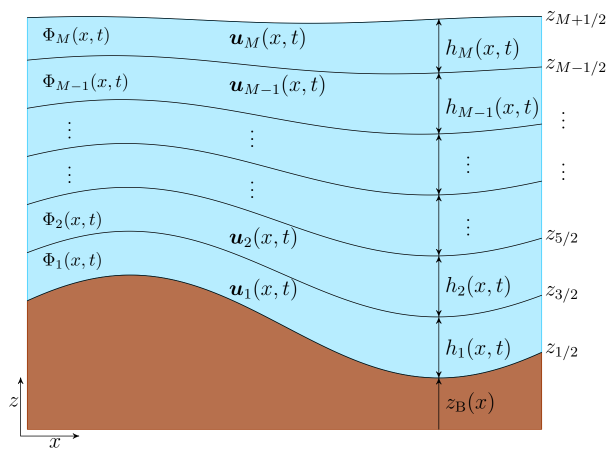


**Fig. 1** Sketch of the multilayer approach

Note that (3.2) and (3.5) allow us to easily change to the original variables. To finish this section, from here so on, the symbol tilde ( $\tilde{}$ ) will be neglected to simplify notation. Thus, the final model in dimensionless variables is given by the dimensionless mass balance equations (3.4) of each solid species and by the dimensionless momentum balance equation of the mixture (3.6)

$$\partial_t(\rho_j\phi_j) + \nabla\cdot(\rho_j\phi_j\boldsymbol{v}_j) = 0, \quad j = 0,\dots,N, \tag{3.8}$$

where

$$\rho_j\phi_j\boldsymbol{v}_j = \rho_j\phi_j\boldsymbol{v} + \frac{1}{\varepsilon}\rho_j f_j^M(\Phi)\boldsymbol{k} - \varepsilon\boldsymbol{I}_\varepsilon^2\boldsymbol{a}_j, \tag{3.9}$$

and dimensionless momentum balance equation of the mixture

$$\partial_t\left(\sum_{j=0}^{N}\rho_j\phi_j\boldsymbol{v}_{\varepsilon,j}\right) + \nabla\cdot\left(\sum_{j=0}^{N}\rho_j\phi_j\boldsymbol{v}_{\varepsilon,j}\otimes\boldsymbol{v}_j\right) = \frac{1}{\varepsilon}\nabla\cdot(\boldsymbol{\Sigma}\tilde{\boldsymbol{I}}) - \frac{1}{\varepsilon}\frac{\rho}{\mathrm{Fr}^2}\boldsymbol{k}. \tag{3.10}$$

## 4 A multilayer approach

### 4.1 Layers, interfaces, and boundaries

For a given final time $T > 0$ and each time $t \in [0,T]$ we denote by $\Omega_{\mathrm{F}}(t)$ the fluid domain and by $I_{\mathrm{F}}(t)$ its projection onto the horizontal plane. To introduce a multilayer system, we divide the fluid domain along the vertical direction into $M \in \mathbb{N}$ layers of thickness $h_\alpha(t,\boldsymbol{x})$ (see Figure 1) with $M+1$ interfaces

$$\Gamma_{\alpha+1/2}(t) = \bigl\{(\boldsymbol{x},z)\in\mathbb{R}^3 : z = z_{\alpha+1/2}(t,\boldsymbol{x}),\, \boldsymbol{x}\in I_{\mathrm{F}}(t)\bigr\}, \quad \alpha = 0,1,\dots,M$$

We assume that the interfaces $\Gamma_{\alpha+1/2}(t)$ are smooth, concretely at least of class $C^1$ in time and space. We denote by $z_{\mathrm{B}} = z_{1/2}$ and $z_{\mathrm{S}} = z_{M+1/2}$ the equations of the bottom and the free surface interfaces $\Gamma_{\mathrm{B}}(t)$ and $\Gamma_{\mathrm{S}}(t)$, respectively. The thickness of layer $\alpha$ at time $t$ and horizontal position $\boldsymbol{x}$ is

$$h_\alpha = h_\alpha(t,\boldsymbol{x}) = z_{\alpha+1/2}(t,\boldsymbol{x}) - z_{\alpha-1/2}(t,\boldsymbol{x}), \quad \alpha = 1,\dots,M,$$

such that $z_{\alpha+1/2} = z_{\mathrm{B}} + h_1 + \dots + h_\alpha$ for $\alpha = 1, \dots, M$. Then the height of the fluid is $h := z_{\mathrm{S}} - z_{\mathrm{B}} = h_1 + \dots + h_M$.

The boundary $\partial\Omega_{\mathrm{F}}(t)$ of $\Omega_{\mathrm{F}}(t)$ can be represented as $\partial\Omega_{\mathrm{F}}(t) = \Gamma_{\mathrm{B}}(t) \cup \Gamma_{\mathrm{S}}(t) \cup \Theta(t)$, where $\Theta(t)$ is the inflow/outflow boundary which we assume here to be vertical. The fluid domain is split as $\overline{\Omega_{\mathrm{F}}(t)} = \cup_{\alpha=1}^M \overline{\Omega_\alpha(t)}$, where we define the layers and their boundaries as

$$\Omega_\alpha(t) := \bigl\{(\boldsymbol{x}, z) \in \mathbb{R}^3 : \boldsymbol{x} \in I_{\mathrm{F}}(t) \text{ and } z_{\alpha-1/2} < z < z_{\alpha+1/2}\bigr\},$$

such that $\partial\Omega_\alpha(t) := \Gamma_{\alpha-1/2}(t) \cup \Gamma_{\alpha+1/2}(t) \cup \Theta_\alpha(t)$, where

$$\Theta_\alpha(t) := \bigl\{(\boldsymbol{x}, z) \in \mathbb{R}^3 : \boldsymbol{x} \in \partial I_{\mathrm{F}}(t) \text{ and } z_{\alpha-1/2} < z < z_{\alpha+1/2}\bigr\}.$$

Hence the inflow/outflow boundary is split as $\overline{\Theta(t)} = \cup_{\alpha=1}^M \overline{\Theta_\alpha(t)}$.

### 4.2 Notation

Based in part on the definition of layers above, we introduce the following notation:

(i) For two tensors $\boldsymbol{a}$ and $\boldsymbol{b}$ of sizes $(n, m)$ and $(n, p)$ respectively, we shall denote by $(\boldsymbol{a};\ \boldsymbol{b})$ the tensor of size $(n, m+p)$ which is the concatenation of $\boldsymbol{a}$ and $\boldsymbol{b}$ in this order.

(ii) For $\boldsymbol{x} = (x_1, \dots, x_{d-1})$ and the differential operator $\nabla = (\partial_{x_1}, \dots, \partial_{x_{d-1}}, \partial_z)$, we define

$$\bar{\nabla} := (\partial_t; \nabla) = (\partial_t, \partial_{x_1}, \dots, \partial_{x_{d-1}}, \partial_z), \quad \nabla_{\boldsymbol{x}} := (\partial_{x_1}, \dots, \partial_{x_{d-1}}).$$

(iii) For $\alpha = 0, 1, \dots, M$ and for a function $f$, we set

$$f^-_{\alpha+1/2} := (f|_{\Omega_\alpha(t)})\big|_{\Gamma_{\alpha+1/2}(t)}, \quad f^+_{\alpha+1/2} := (f|_{\Omega_{\alpha+1}(t)})\big|_{\Gamma_{\alpha+1/2}(t)}.$$

If $f$ is continuous across $\Gamma_{\alpha+1/2}(t)$, we simply set $f_{\alpha+1/2} := f|_{\Gamma_{\alpha+1/2}(t)}$. We shall also use the notation

$$\tilde{f}_{\alpha+1/2} := \frac{1}{2}\bigl(f^+_{\alpha+1/2} + f^-_{\alpha+1/2}\bigr).$$

(iv) We denote by $\boldsymbol{\eta}_{\alpha+1/2}$ the spatial unit normal vector to the interface $\Gamma_\alpha(t)$ outward to the layer $\Omega_\alpha(t)$ for a given time $t$, that is

$$\boldsymbol{\eta}_{\alpha+1/2} := \frac{1}{\sqrt{1 + |\nabla_{\boldsymbol{x}} z_{\alpha+1/2}|^2}} (\nabla_{\boldsymbol{x}} z_{\alpha+1/2}, -1)^{\mathrm{T}}, \quad \alpha = 0, \dots, M.$$

Furthermore, $\boldsymbol{\eta}_{t,\alpha+1/2}$ denotes the (space-time) unit normal vector $\Gamma_\alpha(t)$ pointing to $\Omega_\alpha(t)$, i.e.,

$$\boldsymbol{\eta}_{t,\alpha+1/2} := \frac{1}{\sqrt{1 + |\nabla_{\boldsymbol{x}} z_{\alpha+1/2}|^2 + (\partial_t z_{\alpha-1/2})^2}} (\partial_t z_{\alpha+1/2}, \nabla_{\boldsymbol{x}} z_{\alpha+1/2}, -1)^{\mathrm{T}}, \quad \alpha = 0, \dots, M.$$

(v) Let $\alpha \in \{1, \dots, M-1\}$, and assume that $y$ is a scalar, vectorial, or tensorial quantity defined in $\Omega_\alpha(t)$ and $\Omega_{\alpha+1}(t)$, such that the one-sided limits of $y$ on either side of $\Gamma_{\alpha+1/2}(t)$, that is

$$y^+_{t,\alpha+1/2} := \lim_{\substack{z \to z_{\alpha+1/2} \\ z > z_{\alpha+1/2}}} y(\boldsymbol{x}, z, t), \quad y^-_{t,\alpha+1/2} := \lim_{\substack{z \to z_{\alpha+1/2} \\ z < z_{\alpha+1/2}}} y(\boldsymbol{x}, z, t),$$

are well defined. Then we denote by $[\![y]\!]_{t,\alpha+1/2}$ the jump of $y$ across $\Gamma_{\alpha+1/2}(t)$, that is,

$$[\![y]\!]_{t,\alpha+1/2} = y^{+}_{t,\alpha+1/2} - y^{-}_{t,\alpha+1/2}.$$

If $y$ does not depend on $z$ within each of the layers $\Omega_\alpha(t)$ and $\Omega_{\alpha+1}(t)$, then this implies

$$[\![y]\!]_{t,\alpha+1/2} = \left(y|_{\Omega_{\alpha+1}(t)} - y|_{\Omega_\alpha(t)}\right)\big|_{\Gamma_{\alpha+1/2}(t)}. \tag{4.1}$$

*Remark 2* If we add the time variable as one more dimension, then the corresponding domain $\Omega_T$ is actually given by $\Omega_T = \{(t,\boldsymbol{x},z) : t \in (0,T], (\boldsymbol{x},z) \in \Omega_{\mathrm{F}}(t)\}$ with $\partial\Omega_T = \Lambda_T \cup \Lambda_1 \cup \Lambda_2$, where $\Lambda_T = \{(t,\boldsymbol{x},z) : t \in (0,T), (\boldsymbol{x},z) \in \partial\Omega_{\mathrm{F}}(t)\}$, $\Lambda_1 = \{0\} \times \Omega_{\mathrm{F}}(0)$, and $\Lambda_2 = \{T\} \times \Omega_{\mathrm{F}}(T)$. Since we integrate over $\Omega_{\mathrm{F}}(t)$, we retain here the boundary $\Lambda_T$ for the computations even if it means cancelling the tests functions over the boundaries $\Lambda_1$ and $\Lambda_2$.

### 4.3 Weak solution with discontinuities

Let us recall the conditions to be satisfied by a piecewise smooth weak solution $(\boldsymbol{v}_0,\dots,\boldsymbol{v}_N,\phi_0,\dots,\phi_N,p_{\mathrm{tot}})$ of (3.8)–(3.10), where $\boldsymbol{v}_j$ is defined by (3.9).

**Definition 1** Assume that the velocities $\boldsymbol{v}_0,\dots,\boldsymbol{v}_N$, the pressure $p_{\mathrm{tot}}$ and the volume fractions $\phi_0,\dots,\phi_N$ are smooth in each $\Omega_\alpha(t)$, but possibly discontinuous across the predetermined hypersurfaces $\Gamma_{\alpha+1/2}(t)$ for $\alpha = 1,\dots,M-1$. Then

$$\boldsymbol{y} := (\boldsymbol{v}_0,\dots,\boldsymbol{v}_N,\phi_0,\dots,\phi_N,p_{\mathrm{tot}}) : \Omega_T \ni (t,\boldsymbol{x},z) \mapsto \boldsymbol{y}(t,\boldsymbol{x},z) \in \mathbb{R}^N \times \mathbb{R}^N \times \mathbb{R}$$

is a *weak solution* of (3.8)–(3.10) if the following conditions hold:

(i) The function $\boldsymbol{y}$ is a standard weak solution of (3.8)–(3.10) in each layer $\Omega_\alpha(t)$, $\alpha = 1,\dots,M$.
(ii) For each $\alpha = 1,\dots,M-1$ and $t \in (0,T]$, the following normal flux jump conditions across the interface $\Gamma_{\alpha+1/2}(t)$ are satisfied: for the conservation of mass equations,

$$\big[\!\big[(\rho_j\phi_j;\rho_j\phi_j\boldsymbol{v}_j)\big]\!\big]_{t,\alpha+1/2} \cdot \boldsymbol{\eta}_{t,\alpha+1/2} = 0 \quad \textit{for all } j = 1,\dots,N, \tag{4.2}$$

and for the momentum conservation law corresponding to equation (3.10),

$$\left[\!\!\left[\left(\sum_{j=0}^{N}\rho_j\phi_j\boldsymbol{v}_{\varepsilon,j};\sum_{j=0}^{N}\rho_j\phi_j\boldsymbol{v}_{\varepsilon,j}\otimes\boldsymbol{v}_j - \frac{1}{\varepsilon}\boldsymbol{\Sigma}\tilde{\boldsymbol{I}}\right)\right]\!\!\right]_{t,\alpha+1/2} \cdot \boldsymbol{\eta}_{t,\alpha+1/2} = 0, \tag{4.3}$$

where

$$\boldsymbol{\Sigma} = -p_{\mathrm{tot}}\boldsymbol{I} + \boldsymbol{T}^{\mathrm{E}}_{\varepsilon} \tag{4.4}$$

is the stress tensor of the mixture and $\boldsymbol{v}_{\varepsilon,j} = \boldsymbol{I}_\varepsilon^{-1}\boldsymbol{v}_j$.

There are some different ways to introduce a multilayer model. In [17] for example, the authors integrate the mass and linear momentum equations inside the each layer to define the multilayer model, while in [11] the multilayer approach is deduced as a particular weak solution of a variational formulation. For $\alpha = 1, \dots, M$ and $j = 0, \dots, N$ we set $\boldsymbol{v}_j|_{\Omega_\alpha(t)} := \boldsymbol{v}_{j,\alpha} := (\boldsymbol{u}_{j,\alpha}, w_{j,\alpha})^{\mathrm{T}}$ where $\boldsymbol{u}_{j,\alpha}$, $w_{j,\alpha}$ are horizontal and vertical velocities respectively, $\phi_{j,\alpha} := \phi_j|_{\Omega_\alpha(t)}$, volumetric concentration of the species $j$ on layer $\alpha$. For $\alpha = 1, \dots, M$, the pressure $p_{\mathrm{tot},\alpha} := p_{\mathrm{tot}}|_{\Omega_\alpha(t)}$ and the mixture velocity of each layer by

$$\boldsymbol{v}_\alpha = \frac{1}{\rho} \sum_{j=0}^{N} \rho_j \phi_{j,\alpha} \boldsymbol{v}_{j,\alpha} = (\boldsymbol{u}_\alpha, w_\alpha), \quad \alpha = 1, \dots, M.$$

In both cases we need to assume that the layer thicknesses are small enough to neglect the dependence of the horizotal velocities and the concentration of each species on the vertical variable inside each layer. This means that

$$\partial_z \boldsymbol{u}_{j,\alpha} = 0, \quad \partial_z \phi_{j,\alpha} = 0. \tag{4.5}$$

Under this assumption the vertical velocity and the (hydrostatic) pressure are piecewise linear in $z$, i.e.,

$$\partial_z w_{j,\alpha} = d_{j,\alpha}(t, \boldsymbol{x}), \quad \partial_z p_{\mathrm{tot},\alpha}(t, \boldsymbol{x}) = g_\alpha(t, \boldsymbol{x}) \tag{4.6}$$

for some smooth functions $d_{j,\alpha}(t, \boldsymbol{x})$, and $g_\alpha(t, \boldsymbol{x})$. In the following section we will also use the notation $\Phi_\alpha := (\phi_{0,\alpha}, \phi_{1,\alpha}, \dots, \phi_{N,\alpha})^{\mathrm{T}}$ and $\bar{\rho}_\alpha := \rho_0 \phi_{0,\alpha} + \rho_1 \phi_{1,\alpha} + \dots + \rho_N \phi_{N,\alpha}$.

### 4.4 Mass and momentum conservation jump conditions

In what follows we analyze the jump conditions (4.2) and (4.3), where (4.5) implies

$$\boldsymbol{u}^+_{j,\alpha-1/2}(t, \boldsymbol{x}) = \boldsymbol{u}^-_{j,\alpha+1/2}(t, \boldsymbol{x}) = \boldsymbol{u}_{j,\alpha}(t, \boldsymbol{x}) \quad \text{and} \quad \phi^+_{j,\alpha-1/2}(t, \boldsymbol{x}) = \phi^-_{j,\alpha+1/2}(t, \boldsymbol{x}) = \phi_{j,\alpha}(t, \boldsymbol{x}). \tag{4.7}$$

We define for the lateral limits of the normal mass flux for species $j$ at the interface $\Gamma_{\alpha+1/2}(t)$ by

$$\begin{aligned} G^+_{j,\alpha+1/2} &:= \rho_j \phi_{j,\alpha+1} \bigl( \partial_t z_{\alpha+1/2} + \boldsymbol{u}^+_{j,\alpha+1/2} \cdot \nabla_{\boldsymbol{x}} z_{\alpha+1/2} - w^+_{j,\alpha+1/2} \bigr), \\ G^-_{j,\alpha+1/2} &:= \rho_j \phi_{j,\alpha} \bigl( \partial_t z_{\alpha+1/2} + \boldsymbol{u}^-_{j,\alpha+1/2} \cdot \nabla_{\boldsymbol{x}} z_{\alpha+1/2} - w^-_{j,\alpha+1/2} \bigr), \quad j = 0, 1, \dots, N. \end{aligned} \tag{4.8}$$

The mass conservation jump conditions (4.2) are then satisfied provided that

$$G_{j,\alpha+1/2} := G^-_{j,\alpha+1/2} = G^+_{j,\alpha+1/2}, \quad j = 0, 1, \dots, N, \tag{4.9}$$

where $G_{j,\alpha+1/2}$ represents the normal mass flux for species $j$ at $\Gamma_{\alpha+1/2}(t)$. Taking into account (4.7), we obtain the structure of the horizontal and vertical velocities

$$\boldsymbol{u}^+_{j,\alpha+1/2} = \boldsymbol{u}_{\alpha+1} - \varepsilon \boldsymbol{a}^+_{\mathrm{h},j,\alpha+1/2} / (\rho_j \phi_{j,\alpha+1}), \qquad \boldsymbol{u}^-_{j,\alpha+1/2} = \boldsymbol{u}_\alpha - \varepsilon \boldsymbol{a}^-_{\mathrm{h},j,\alpha+1/2} / (\rho_j \phi_{j,\alpha}), \tag{4.10}$$

$$w^\pm_{j,\alpha+1/2} = w^\pm_{\alpha+1/2} + (\rho_j f^\pm_{j,\alpha+1/2} - a^\pm_{3,j,\alpha+1/2}) / (\varepsilon \rho_j \phi^\pm_{j,\alpha+1/2}), \tag{4.11}$$

where $f^\pm_{j,\alpha+1/2}$ and $\varepsilon \boldsymbol{I}^2_\varepsilon \boldsymbol{a}^\pm_{j,\alpha+1/2}$ must satisfy the respective condition

$$\sum_{j=0}^{N} \rho_j f^\pm_{j,\alpha+1/2} = 0, \quad \sum_{j=0}^{N} \varepsilon \boldsymbol{I}^2_\varepsilon \boldsymbol{a}^\pm_{j,\alpha+1/2} = \boldsymbol{0}.$$

We can then compute the total normal mass flux across $\Gamma_{\alpha+1/2}(t)$ as $G_{\alpha+1/2} := \sum_{j=0}^{N} G_{j,\alpha+1/2}$, and by (4.8) and (4.9) we get the jump condition

$$G_{\alpha+1/2} = G^-_{\alpha+1/2} = G^+_{\alpha+1/2}, \tag{4.12}$$

for the first equation from (2.3), where

$$\begin{aligned} G^+_{\alpha+1/2} &:= \bar{\rho}_{\alpha+1}\bigl(\partial_t z_{\alpha+1/2} + \boldsymbol{u}_{\alpha+1} \cdot \nabla_{\boldsymbol{x}} z_{\alpha+1/2} - w^+_{\alpha+1/2}\bigr),\\ G^-_{\alpha+1/2} &:= \bar{\rho}_{\alpha}\bigl(\partial_t z_{\alpha+1/2} + \boldsymbol{u}_{\alpha} \cdot \nabla_{\boldsymbol{x}} z_{\alpha+1/2} - w^-_{\alpha+1/2}\bigr). \end{aligned} \tag{4.13}$$

Then, after substituting the limits of the horizontal and vertical velocities (4.10) and (4.11) into (4.8) and using the definition of limits of total normal mass flux (4.13) and the jump condition (4.12), we get

$$\begin{aligned} G^+_{j,\alpha+1/2} &= \frac{\rho_j \phi_{j,\alpha+1}}{\bar{\rho}_{\alpha+1}} G_{\alpha+1/2} - \frac{1}{\varepsilon}\rho_j f^+_{j,\alpha+1/2} - \varepsilon \boldsymbol{I}^2_\varepsilon \boldsymbol{a}^+_{j,\alpha+1/2} \cdot \boldsymbol{\eta}_{\alpha+1/2}\sqrt{1 + |\nabla_{\boldsymbol{x}} z_{\alpha+1/2}|^2},\\ G^-_{j,\alpha+1/2} &= \frac{\rho_j \phi_{j,\alpha}}{\bar{\rho}_{\alpha}} G_{\alpha+1/2} - \frac{1}{\varepsilon}\rho_j f^-_{j,\alpha+1/2} - \varepsilon \boldsymbol{I}^2_\varepsilon \boldsymbol{a}^-_{j,\alpha+1/2} \cdot \boldsymbol{\eta}_{\alpha+1/2}\sqrt{1 + |\nabla_{\boldsymbol{x}} z_{\alpha+1/2}|^2}. \end{aligned} \tag{4.14}$$

The relationship between normal mass flux of species $j$ and the total normal mass flux across $\Gamma_{\alpha+1/2}(t)$ is computed using the $j$-th mass jump condition (4.9) and summing for each $j = 0, \dots, N$ the equations from (4.14). This yields

$$G_{j,\alpha+1/2} = \tilde{\phi}_{j,\alpha+1/2} G_{\alpha+1/2} - \frac{1}{\varepsilon}\rho_j \tilde{f}_{j,\alpha+1/2} - \varepsilon \boldsymbol{I}^2_\varepsilon \tilde{\boldsymbol{a}}_{j,\alpha+1/2} \cdot \boldsymbol{\eta}_{\alpha+1/2}\sqrt{1 + |\nabla_{\boldsymbol{x}} z_{\alpha+1/2}|^2}, \tag{4.15}$$

where for each $j = 0, \dots, N$ the averages $\tilde{\phi}_{j,\alpha+1/2}$, $\tilde{f}_{j,\alpha+1/2}$ and $\tilde{\boldsymbol{a}}_{j,\alpha+1/2}$ are given by

$$\begin{aligned} &\tilde{\phi}_{j,\alpha+1/2} := \frac{1}{2}\left(\frac{\rho_j \phi_{j,\alpha+1}}{\bar{\rho}_{\alpha+1}} + \frac{\rho_j \phi_{j,\alpha}}{\bar{\rho}_{\alpha}}\right), \quad \tilde{f}_{j,\alpha+1/2} := \frac{1}{2}\bigl(f^+_{j,\alpha+1/2} + f^-_{j,\alpha+1/2}\bigr),\\ &\tilde{\boldsymbol{a}}_{j,\alpha+1/2} := \frac{1}{2}\bigl(\boldsymbol{a}^+_{j,\alpha+1/2} + \boldsymbol{a}^-_{j,\alpha+1/2}\bigr). \end{aligned} \tag{4.16}$$

On the other hand, setting $\boldsymbol{M} = \varepsilon \tilde{\boldsymbol{I}}^{-1}$ and writing the jump condition of species $j$ as

$$\begin{aligned} &\bigl[\!\bigl[(\rho_j \phi_j \boldsymbol{v}_{\varepsilon,j}; \rho_j \phi_j \boldsymbol{v}_{\varepsilon,j} \otimes \boldsymbol{v}_j)\bigr]\!\bigr]_{t,\alpha+1/2} \cdot (\partial_t z_{\alpha+1/2}, \nabla_{\boldsymbol{x}} z_{\alpha+1/2}, -1)^{\mathrm{T}}\\ &= G_{j,\alpha+1/2} \boldsymbol{M} [\![\boldsymbol{v}_j]\!]_{t,\alpha+1/2}, \quad j = 0, 1, \dots, N, \end{aligned}$$

where $[\![(\dots;\dots)]\!]$ is a matricial $3 \times 4$ jump, we may rewrite the momentum jump condition (4.3) as

$$\frac{1}{\varepsilon}[\![\boldsymbol{\Sigma}\tilde{\boldsymbol{I}}]\!]_{t,\alpha+1/2} \cdot \boldsymbol{\eta}_{\alpha+1/2} = \frac{1}{\sqrt{1 + |\nabla_{\boldsymbol{x}} z_{\alpha+1/2}|^2}} \sum_{j=0}^{N} G_{j,\alpha+1/2} \boldsymbol{M} [\![\boldsymbol{v}_j]\!]_{t,\alpha+1/2}. \tag{4.17}$$

Now, from the left-hand side of (4.17) it is clear that we need to define an approximation of the stress tensor at each interface $\Gamma_{\alpha+1/2}$. Then, for $\alpha = 1, \dots, M-1$, the stress tensor from (4.4) is decomposed as

$$\boldsymbol{\Sigma}^{\pm}_{\alpha+1/2} = -p_{\mathrm{tot},\alpha+1/2}\boldsymbol{I} + \boldsymbol{T}^{\mathrm{E},\pm}_{\varepsilon,\alpha+1/2}, \tag{4.18}$$

where $p_{\mathrm{tot},\alpha+1/2}$ is the pressure and $\boldsymbol{T}^{\mathrm{E},\pm}_{\varepsilon,\alpha+1/2}$ are the limit approximations of the viscous stress tensor $\boldsymbol{T}^{\mathrm{E}}_{\varepsilon}$ at $\Gamma_{\alpha+1/2}$. From (4.17) we deduce that

$$\frac{1}{\varepsilon}\left(\boldsymbol{T}^{\mathrm{E},+}_{\varepsilon,\alpha+1/2}-\boldsymbol{T}^{\mathrm{E},-}_{\varepsilon,\alpha+1/2}\right)\tilde{\boldsymbol{I}}\,\boldsymbol{\eta}_{\alpha+1/2}=\frac{1}{\sqrt{1+|\nabla_{\boldsymbol{x}}z_{\alpha+1/2}|^2}}\sum_{j=0}^{N}G_{j,\alpha+1/2}\boldsymbol{M}[\![\boldsymbol{v}_j]\!]_{t,\alpha+1/2}, \tag{4.19}$$

where $\boldsymbol{T}^{\mathrm{E},\pm}_{\varepsilon,\alpha+1/2}$ should be defined such that

$$\tilde{\boldsymbol{T}}^{\mathrm{E}}_{\alpha+1/2}:=\frac{1}{2}\left(\boldsymbol{T}^{\mathrm{E},+}_{\varepsilon,\alpha+1/2}+\boldsymbol{T}^{\mathrm{E},-}_{\varepsilon,\alpha+1/2}\right)$$

is an approximation of the viscous stress tensor $\boldsymbol{T}^{\mathrm{E}}_{\varepsilon}|_{\Gamma_{\alpha+1/2}}$. Then, as in [11] we define

$$\tilde{\boldsymbol{T}}^{\mathrm{E}}_{\alpha+1/2}=\frac{\eta}{2}\tilde{\boldsymbol{D}}_{\varepsilon,\alpha+1/2}+2\varepsilon\lambda(\tilde{\nabla}\cdot\tilde{\boldsymbol{v}})_{\alpha+1/2}\boldsymbol{I} \tag{4.20}$$

with

$$\tilde{\boldsymbol{D}}_{\varepsilon,\alpha+1/2}=\begin{bmatrix}\varepsilon\boldsymbol{D}_{\varepsilon,\mathrm{h}}(\tilde{\boldsymbol{u}}_{\mathrm{h},\alpha+1/2}) & \varepsilon^2(\nabla_{\boldsymbol{x}}\tilde{w}_{\alpha+1/2})^{\mathrm{T}}+\boldsymbol{Q}_{\mathrm{h},\alpha+1/2}\\ \varepsilon^2\nabla_{\boldsymbol{x}}\tilde{w}_{\alpha+1/2}+(\boldsymbol{Q}_{\mathrm{h},\alpha+1/2})^{\mathrm{T}} & 2\varepsilon Q_{\mathrm{v},\alpha+1/2}\end{bmatrix}, \tag{4.21}$$

$$(\tilde{\nabla}\cdot\tilde{\boldsymbol{v}})_{\alpha+1/2}=\nabla_{\boldsymbol{x}}\cdot\tilde{\boldsymbol{u}}_{\mathrm{h},\alpha+1/2}+Q_{\mathrm{v},\alpha+1/2}, \tag{4.22}$$

where $\boldsymbol{Q}_{\alpha+1/2}=\boldsymbol{Q}(\boldsymbol{v})|_{\Gamma_{\alpha+1/2}}$ and $\boldsymbol{Q}=(\boldsymbol{Q}_{\mathrm{h}},Q_{\mathrm{v}})^{\mathrm{T}}$ satisfies the equation $\boldsymbol{Q}-\partial_z\boldsymbol{v}=\boldsymbol{0}$. To approximate $\boldsymbol{Q}$, the solution of this equation, we approximate $\boldsymbol{v}$ by a linear interpolation in $z$, named as $\tilde{\boldsymbol{v}}$, such that

$$\tilde{\boldsymbol{v}}|_{z=\frac{1}{2}(z_{\alpha-1/2}+z_{\alpha+1/2})}=\boldsymbol{v}_{\alpha}.$$

Finally, introducing $\tilde{\boldsymbol{T}}^{\mathrm{E}}_{\alpha+1/2}$ in the equality (4.19) we get

$$\boldsymbol{T}^{\mathrm{E},\pm}_{\varepsilon,\alpha+1/2}\tilde{\boldsymbol{I}}\,\boldsymbol{\eta}_{\alpha+1/2}=\tilde{\boldsymbol{T}}^{\mathrm{E}}_{\alpha+1/2}\tilde{\boldsymbol{I}}\,\boldsymbol{\eta}_{\alpha+1/2}\pm\frac{1}{2}\frac{\varepsilon}{\sqrt{1+|\nabla_{\boldsymbol{x}}z_{\alpha+1/2}|^2}}\sum_{j=0}^{N}G_{j,\alpha+1/2}\boldsymbol{M}[\![\boldsymbol{v}_j]\!]_{t,\alpha+1/2}, \tag{4.23}$$

which satisfies the jump condition (4.17).

### 4.5 Vertical velocity of the mixture

It is well known that in the multilayer approach under hydrostatic pressure the vertical velocity disappears from the third equation of the momentum equations so we need to recover this velocity by post-processing data. In [11] we compute vertical velocities of each species and vertical velocity of the mixture, but the former are only computed to get the vertical velocity of the mixture. In other words, it is not possible to use the vertical velocities of each species to determin the velocity of the each species, since these velocities are not well defined for all $t\in[0,T]$. On the other hand, these particular velocities are important and they allow us to compute the vertical velocity of the mixture for all $t\in[0,T]$.

So, to compute the vertical velocities of each species we set $\alpha\in\{1,\dots,M\}$ and integrate vertically the mass balance equations (3.8) over a layer $\alpha$, this is over $(z_{\alpha-1/2},z)$ for $z\in(z_{\alpha-1/2},z_{\alpha+1/2})$ and then we use the assumption (4.5) to get for $j=0,\dots,N$

$$\partial_t(\rho_j\phi_{j,\alpha})(z-z_{\alpha-1/2})+\nabla_{\boldsymbol{x}}\cdot(\rho_j\phi_{j,a}\boldsymbol{u}_{j,\alpha})(z-z_{\alpha-1/2})+\rho_j\phi_{j,\alpha}\big(w_{j,\alpha}(t,\boldsymbol{x},z)-w^{+}_{j,\alpha-1/2}\big)=0, \tag{4.24}$$

where it is clear from (4.24) that it is not possible to recover the vertical velocity of species $j$ when $\phi_{j,\alpha} = 0$. On the other hand, if we sum all equations in (4.24) from $j = 0$ to $j = N$ we get an expression for the vertical velocity of the mixture

$$w_\alpha(t, \boldsymbol{x}, z) = w^+_{\alpha-1/2} - \frac{1}{\bar{\rho}_\alpha}\big(\partial_t \bar{\rho}_\alpha + \nabla_{\boldsymbol{x}} \cdot (\bar{\rho}_\alpha \boldsymbol{u}_\alpha)\big)(z - z_{\alpha-1/2}), \tag{4.25}$$

where $w^+_{\alpha-1/2}$ is defined by using the mass jump condition (4.12), so this vertical velocity is given by

$$w^+_{\alpha-1/2} = \frac{1}{\bar{\rho}_\alpha}\big((\bar{\rho}_\alpha - \bar{\rho}_{\alpha-1})\partial_t z_{\alpha-1/2} + (\bar{\rho}_\alpha \boldsymbol{u}_\alpha - \bar{\rho}_{\alpha-1}\boldsymbol{u}_{\alpha-1}) \cdot \nabla_{\boldsymbol{x}} z_{\alpha-1/2} + \bar{\rho}_{\alpha-1} w^-_{\alpha-1/2}\big),$$

and the corresponding limit of the vertical velocity $w^-_{\alpha-1/2}$ at the interface $\Gamma_{\alpha-1/2}(t)$ is computed using the linear profile (4.25) in layer $\alpha - 1$ evaluated at $z_{\alpha-1/2}$:

$$w^-_{\alpha-1/2} = w^+_{\alpha-3/2} - \frac{h_{\alpha-1}}{\bar{\rho}_{\alpha-1}}\big(\partial_t(\bar{\rho}_{\alpha-1}) + \nabla_{\boldsymbol{x}} \cdot (\bar{\rho}_{\alpha-1}\boldsymbol{u}_{\alpha-1})\big).$$

Finally, the vertical velocities of the mixture in each layer are computed recursively as follows. First, the vertical velocity $w^+_{1/2}$ is computed using mass transference condition (4.13) at the bottom by

$$w^+_{1/2} = \partial_t z_{\mathrm{B}} + \boldsymbol{u}_1 \cdot \nabla_{\boldsymbol{x}} z_{\mathrm{B}} - \frac{G_{1/2}}{\rho_1}.$$

Then, for $\alpha = 1, \dots, N$ and $z \in (z_{\alpha-1/2}, z_{\alpha+1/2})$ we obtain the vertical velocities of the mixture in each layer successively as

$$\begin{aligned}
w_\alpha(t, \boldsymbol{x}, z) &= w^+_{\alpha-1/2} - \frac{1}{\bar{\rho}_\alpha}\big(\partial_t \bar{\rho}_\alpha + \nabla_{\boldsymbol{x}} \cdot (\bar{\rho}_\alpha \boldsymbol{u}_\alpha)\big)(z - z_{\alpha-1/2}), \\
w^-_{\alpha+1/2} &= w^+_{\alpha-1/2} - \frac{h_\alpha}{\bar{\rho}_\alpha}\big(\partial_t \bar{\rho}_\alpha + \nabla_{\boldsymbol{x}} \cdot (\bar{\rho}_\alpha \boldsymbol{u}_\alpha)\big), \\
w^+_{\alpha+1/2} &= \frac{1}{\bar{\rho}_{\alpha+1}}\big((\bar{\rho}_{\alpha+1} - \bar{\rho}_\alpha)\partial_t z_{\alpha+1/2} + (\bar{\rho}_{\alpha+1}\boldsymbol{u}_{\alpha+1} - \bar{\rho}_\alpha \boldsymbol{u}_\alpha) \cdot \nabla_{\boldsymbol{x}} z_{\alpha+1/2} + \bar{\rho}_\alpha w^-_{\alpha+1/2}\big).
\end{aligned}$$

## 5 Multilayer approach

Following [11, 16], we now derive the multilayer model using the final form of the dimensionless model (3.8), (3.9), (3.10). We first need to introduce the multilayer version of the hydrostatic pressure.

### 5.1 Multilayer version of hydrostatic pressure

Using the last equality of the linear momentum equation of the mixture (3.10) we get

$$\partial_z p_{\mathrm{tot}} = -\frac{\rho}{\mathrm{Fr}^2} + \varepsilon\left(\nabla_x \cdot \left(\frac{\eta}{2}\partial_z \boldsymbol{v}_{\mathrm{h}}\right) + \partial_z(\eta \partial_z w) + \partial_z(2\lambda \nabla \cdot \boldsymbol{v})\right) + \mathcal{O}(\varepsilon^2).$$

To recover the hydrostatic framework (assumption (4.6)) we neglect in this equation up to $\mathcal{O}(\varepsilon)$ terms, which yields $\partial_z p_{\mathrm{tot}} = -\rho/\mathrm{Fr}^2$. Then the multilayer version of the pressure is given by

$$p_{\mathrm{tot},\alpha} = p_{\alpha+1/2} + \bar{\rho}_\alpha \frac{z_{\alpha+1/2} - z}{\mathrm{Fr}^2}, \quad p_{\alpha+1/2} = p_{\mathrm{S}} + \sum_{\beta=\alpha+1}^{M} \frac{\bar{\rho}_\beta h_\beta}{\mathrm{Fr}^2}, \tag{5.1}$$

where the component $p_{\alpha+1/2}$ is the pressure at interface $\Gamma_{\alpha+1/2}(t)$, $p_{\mathrm{S}}$ denotes the pressure at the free surface and Fr is the Froude number. This assumption on pressure ensures that the pressure is not an unknown of the problem.

### 5.2 Weak formulation

The multilayer approach arises from a variational formulation of the system (3.8)–(3.10). We notice that the multilayer model is a particular weak solution of these variational identities. The weak formulation in $\Omega_\alpha(t)$ for $\alpha = 1, \dots, N$ is as follows (cf. [11]). Assume that $\boldsymbol{v}_{j,\alpha} \in L^2(0,T; H^1(\Omega_\alpha(t))^3)$, $\partial_t \boldsymbol{v}_{j,\alpha} \in L^2(0,T; L^2(\Omega_\alpha(t))^3)$, $\phi_{j,\alpha} \in L^2(0,T; H^1(\Omega_\alpha(t)))$, $\partial_t \phi_{j,\alpha} \in L^2(0,T; L^2(\Omega_\alpha(t)))$ and $p_{\mathrm{tot},\alpha} \in L^2(0,T; H^1(\Omega_\alpha(t)))$. Then a weak solution $(\boldsymbol{v}_{j,\alpha}, \phi_{j,\alpha}, p_{\mathrm{tot},\alpha})$ in $\Omega_\alpha(t)$ should satisfy for all $\varphi \in L^2(\Omega_\alpha(t))$ and for all $\boldsymbol{\vartheta} \in H^1(\Omega_\alpha(t))^3$ with $\boldsymbol{\vartheta}|_{\partial I_{\mathrm{F}}} = 0$ the identities

$$\begin{aligned} & \int_{\Omega_\alpha(t)} \bigl(\partial_t(\rho_j \phi_{j,\alpha}) + \nabla \cdot (\rho_j \phi_{j,\alpha} \boldsymbol{v}_{j,\alpha})\bigr) \varphi \, \mathrm{d}\Omega = 0, \\ & \int_{\Omega_\alpha(t)} \left( \sum_{j=0}^{N} \rho_j \partial_t (\phi_{j,\alpha} \boldsymbol{v}_{\varepsilon,j,\alpha}) \right) \cdot \boldsymbol{\vartheta} \, \mathrm{d}\Omega + \int_{\Omega_\alpha(t)} \left( \sum_{j=0}^{N} \rho_j \nabla \cdot (\phi_{j,\alpha} \boldsymbol{v}_{\varepsilon,j,\alpha} \otimes \boldsymbol{v}_{j,\alpha}) \right) \cdot \boldsymbol{\vartheta} \, \mathrm{d}\Omega \\ & + \frac{1}{\varepsilon} \int_{\Omega_\alpha(t)} (\boldsymbol{T}^{\mathrm{E}}_{\varepsilon,\alpha} \tilde{\boldsymbol{I}}) : \nabla \boldsymbol{\vartheta} \, \mathrm{d}\Omega - \frac{1}{\varepsilon} \int_{\Omega_\alpha(t)} (p_{\mathrm{tot},\alpha} \tilde{\boldsymbol{I}}) : \nabla \boldsymbol{\vartheta} \, \mathrm{d}\Omega + \frac{1}{\varepsilon} \int_{\Gamma_{\alpha+1/2}(t)} (\boldsymbol{\Sigma}^-_{\alpha+1/2} \tilde{\boldsymbol{I}}) \boldsymbol{\eta}_{\alpha+1/2} \cdot \boldsymbol{\vartheta} \, \mathrm{d}\Gamma \\ & - \frac{1}{\varepsilon} \int_{\Gamma_{\alpha-1/2}(t)} (\boldsymbol{\Sigma}^+_{\alpha-1/2} \tilde{\boldsymbol{I}}) \boldsymbol{\eta}_{\alpha-1/2} \cdot \boldsymbol{\vartheta} \, \mathrm{d}\Gamma = -\frac{1}{\varepsilon} \int_{\Omega_\alpha(t)} \frac{g}{\mathrm{Fr}^2} \bar{\rho}_\alpha \boldsymbol{k} \cdot \boldsymbol{\vartheta} \, \mathrm{d}\Omega, \end{aligned} \tag{5.2}$$

for particular test functions $\varphi$ and $\boldsymbol{\vartheta}$ that satisfy $\partial_z \varphi = 0$ and

$$\boldsymbol{\vartheta}(t, \boldsymbol{x}, z) = \bigl(\boldsymbol{\vartheta}_{\mathrm{h}}(t, \boldsymbol{x}), (z - z_{\mathrm{B}}) \mathcal{V}(t, \boldsymbol{x})\bigr)^{\mathrm{T}}, \tag{5.3}$$

where $\boldsymbol{\vartheta}_{\mathrm{h}}$ and $\mathcal{V}$ are smooth functions that do not depend on $z$. We use the structure given by (4.5), (4.6) and apply straightforward calculations analogous to those of [11, Appendix C] (details are omitted here).

Then we arrive at the following multilayer version of (3.8)–(3.10):

$$
\begin{aligned}
&\text{For } \alpha = 0,\dots,M:\\
&\partial_t(\rho_j\phi_{j,\alpha}h_\alpha) + \nabla_{\boldsymbol{x}}\cdot(\rho_j\phi_{j,\alpha}h_\alpha\boldsymbol{u}_{j,\alpha}) = G_{j,\alpha+1/2} - G_{j,\alpha-1/2}, \quad j=0,1,\dots,N,\\
&\sum_{j=0}^{N}\Big(\rho_j h_\alpha \partial_t\big(\phi_{j,\alpha}\boldsymbol{u}_{j,\alpha}\big) + \rho_j h_\alpha \nabla_{\boldsymbol{x}}\cdot\big(\phi_{j,\alpha}\boldsymbol{u}_{j,\alpha}\otimes\boldsymbol{u}_{j,\alpha}\big) + \rho_j\phi_{j,\alpha}\big(w^-_{j,\alpha+1/2} - w^+_{j,\alpha-1/2}\big)\boldsymbol{u}_{j,\alpha}\Big)\\
&+\int_{z_{\alpha-1/2}}^{z_{\alpha+1/2}}\nabla_{\boldsymbol{x}}p_{\mathrm{tot},\alpha}\,\mathrm{d}z - \boldsymbol{\nabla}_{\boldsymbol{x}}\cdot\big(h_\alpha\boldsymbol{T}^{\mathrm{E}}_{\mathrm{h},\alpha}\big) + \tilde{\boldsymbol{T}}^{\mathrm{E}}_{\mathrm{h},\alpha+1/2}(\nabla_{\boldsymbol{x}}z_{\alpha+1/2})^{\mathrm{T}} - \frac{1}{\varepsilon}\tilde{\boldsymbol{T}}^{\mathrm{E}}_{\boldsymbol{x}z,\alpha+1/2}\\
&-\tilde{\boldsymbol{T}}^{\mathrm{E}}_{\mathrm{h},\alpha-1/2}(\nabla_{\boldsymbol{x}}z_{\alpha-1/2})^{\mathrm{T}} + \frac{1}{\varepsilon}\tilde{\boldsymbol{T}}^{\mathrm{E}}_{\boldsymbol{x}z,\alpha-1/2}\\
&= \frac{1}{2}\sum_{j=0}^{N}G_{j,\alpha+1/2}(\boldsymbol{u}_{j,\alpha+1}-\boldsymbol{u}_{j,\alpha}) + \frac{1}{2}\sum_{j=0}^{N}G_{j,\alpha-1/2}(\boldsymbol{u}_{j,\alpha}-\boldsymbol{u}_{j,\alpha-1}),
\end{aligned}
\tag{5.4}
$$

where the mass transfer terms $G_{j,\alpha+1/2}$ are given by (4.15), the horizontal and vertical velocities $\boldsymbol{u}_{j,\alpha}$ and $w^{\pm}_{\alpha+1/2}$ are given by (4.10) and (4.11), respectively, where we keep in mind the equalities (4.7), and the viscous stress terms are given by (4.20)–(4.22), and the integral term of (5.4) by

$$
\int_{z_{\alpha-1/2}}^{z_{\alpha+1/2}}\nabla_{\boldsymbol{x}}p_{\mathrm{tot},\alpha}\,\mathrm{d}z = h_\alpha\left(\nabla_{\boldsymbol{x}}\bar{p}_\alpha + \frac{\rho_\alpha}{\mathrm{Fr}^2}\nabla_{\boldsymbol{x}}\bar{z}_\alpha\right),
$$

where $\bar{p}_\alpha$ and $\bar{z}_\alpha$ are defined as

$$
\bar{p}_\alpha := p_{\mathrm{S}} + \sum_{\beta=\alpha+1}^{M}\rho_\beta h_\beta/\mathrm{Fr}^2 + \rho_\alpha\frac{h_\alpha}{2\mathrm{Fr}^2}, \quad \bar{z}_\alpha := z_{\mathrm{B}} + \sum_{\beta=1}^{\alpha-1}h_\beta + \frac{h_\alpha}{2}. \tag{5.5}
$$

To this point all equations were given in dimensionless variables. In Section 5.3 and from here so on we will return to the original variables.

### 5.3 Multilayer model in original variables

To obtain the final form of the model, first we multiply the mass and linear momentum balance equations (5.4) by $\varepsilon := H/L$, and discard all $\mathcal{O}(\varepsilon^2)$ terms. Finally we use (3.3) and (3.5) to return to the original variables. Multiplying (4.10) and (4.11) by $\varepsilon$ and neglecting small terms, we obtain $\boldsymbol{u}_{j,\alpha} = \boldsymbol{u}_\alpha$. Analogously for (4.15) we get

$$
G_{j,\alpha+1/2} = \tilde{\phi}_{j,\alpha+1/2}G_{\alpha+1/2} - \rho_j\tilde{f}_{j,\alpha+1/2} + \tilde{a}_{3,j,\alpha+1/2}. \tag{5.6}
$$

For the viscous stress tensor from (3.7) we have

$$
\boldsymbol{T}^{\mathrm{E}}_{\varepsilon}(\boldsymbol{v})\tilde{\boldsymbol{I}} = \frac{\eta}{2}\begin{bmatrix}\varepsilon^2\boldsymbol{D}_{\varepsilon,\mathrm{h}}(\boldsymbol{v}) & \partial_z\boldsymbol{v}_{\mathrm{h}} + \varepsilon^2(\nabla_x w)^{\mathrm{T}}\\ \varepsilon((\partial_z\boldsymbol{v}_{\mathrm{h}})^{\mathrm{T}} + \varepsilon^2\nabla_x w) & 2\varepsilon\partial_z w\end{bmatrix} + 2\lambda(\nabla\cdot\boldsymbol{v})\begin{bmatrix}\varepsilon^2 & 0 & 0\\ 0 & \varepsilon^2 & 0\\ 0 & 0 & \varepsilon\end{bmatrix},
$$

along with an analogous expression for the approximation of the viscous stress tensor at each interface $\tilde{\boldsymbol{T}}^{\mathrm{E}}_{\alpha+1/2}(\boldsymbol{v})$. So the multilayer approach in original variables is given by

$$
\begin{aligned}
&\text{For } \alpha = 1,\dots,M:\\
&\partial_t(\rho_j\phi_{j,\alpha}h_\alpha) + \nabla_{\boldsymbol{x}}\cdot(\rho_j\phi_{j,\alpha}h_\alpha\boldsymbol{u}_\alpha)\\
&= \tilde{\phi}_{j,\alpha+1/2}G_{\alpha+1/2} - \tilde{\phi}_{j,\alpha-1/2}G_{\alpha-1/2}\\
&\quad - \rho_j(\tilde{f}_{j,\alpha+1/2} - \tilde{f}_{j,\alpha-1/2}) + \tilde{a}_{j,3,\alpha+1/2} - \tilde{a}_{j,3,\alpha-1/2}, \quad j = 0,\dots,N,\\
&h_\alpha\partial_t\bigl(\bar{\rho}_\alpha\boldsymbol{u}_\alpha\bigr) + h_\alpha\nabla_{\boldsymbol{x}}\cdot\bigl(\bar{\rho}_\alpha\boldsymbol{u}_\alpha\otimes\boldsymbol{u}_\alpha\bigr) + \sum_{j=0}^{N}\rho_j\phi_{j,\alpha}\bigl(w^-_{j,\alpha+1/2} - w^+_{j,\alpha-1/2}\bigr)\boldsymbol{u}_\alpha\\
&+ h_\alpha\bigl(\nabla_{\boldsymbol{x}}\bar{p}_\alpha + g\rho_\alpha\nabla_{\boldsymbol{x}}\bar{z}_\alpha\bigr)\\
&= \frac{1}{2}G_{\alpha+1/2}(\boldsymbol{u}_{\alpha+1} - \boldsymbol{u}_\alpha) + \frac{1}{2}G_{\alpha-1/2}(\boldsymbol{u}_\alpha - \boldsymbol{u}_{\alpha-1}) + \boldsymbol{K}_{\alpha+1/2} - \boldsymbol{K}_{\alpha-1/2},
\end{aligned}
\tag{5.7}
$$

where the mass transfer terms $G_{\alpha+1/2}$ through each interface $\mathit{\Gamma}_{\alpha+1/2}$ for $\alpha = 0,\dots,M$ are given by (4.12) and (4.13), and $\tilde{\phi}_{j,\alpha+1/2}$, $\tilde{f}_{j,\alpha+1/2}$, and $\tilde{a}_{j,3,\alpha+1/2}$ are given by (4.16). The terms $\boldsymbol{K}_{\alpha+1/2}$ are the viscous stress tensors that remain after discarding small terms. These terms are given by

$$
\boldsymbol{K}_{\alpha+1/2} = \frac{\eta}{2}\boldsymbol{Q}_{\mathrm{h},\alpha+1/2}, \quad \alpha = 1,\dots,M. \tag{5.8}
$$

The total mass equation of the mixture at layer $\alpha$ can be recovered summing from $j = 0$ to $j = N$ the first equations of (5.7). This yields

$$
\partial_t(\bar{\rho}_\alpha h_\alpha) + \nabla_{\boldsymbol{x}}\cdot(\bar{\rho}_\alpha h_\alpha\boldsymbol{u}_\alpha) = G_{\alpha+1/2} - G_{\alpha-1/2}, \quad \alpha = 1,\dots,M. \tag{5.9}
$$

The third term of the linear momentum balance in (5.7) can be written as follows, where we use (4.25) evaluated at $z_{\alpha+1/2}$:

$$
\bar{\rho}_\alpha(w^-_{\alpha+1/2} - w^+_{\alpha-1/2}) = -h_\alpha\bigl(\partial_t\bar{\rho}_\alpha + \nabla_{\boldsymbol{x}}\cdot(\bar{\rho}_\alpha\boldsymbol{u}_\alpha)\bigr), \quad \alpha = 1,\dots,M. \tag{5.10}
$$

Finally, multiplying (5.10) by $\boldsymbol{u}_\alpha$ and introducing the result into the momentum equation of (5.7) and using (5.9) multiplied by $\boldsymbol{u}_\alpha$, we get the final form of the multilayer model

$$
\begin{aligned}
&\text{For } \alpha = 1,\dots,M:\\
&\partial_t(\rho_j\phi_{j,\alpha}h_\alpha) + \nabla_{\boldsymbol{x}}\cdot(\rho_j\phi_{j,\alpha}h_\alpha\boldsymbol{u}_\alpha)\\
&= \tilde{\phi}_{j,\alpha+1/2}G_{\alpha+1/2} - \tilde{\phi}_{j,\alpha-1/2}G_{\alpha-1/2}\\
&\quad - \rho_j(\tilde{f}_{j,\alpha+1/2} - \tilde{f}_{j,\alpha-1/2}) + \tilde{a}_{j,3,\alpha+1/2} - \tilde{a}_{j,3,\alpha-1/2}, \quad j = 0,\dots,N,\\
&\partial_t(h_\alpha\bar{\rho}_\alpha\boldsymbol{u}_\alpha) + \nabla_{\boldsymbol{x}}\cdot\bigl(h_\alpha\bar{\rho}_\alpha\boldsymbol{u}_\alpha\otimes\boldsymbol{u}_\alpha\bigr) + h_\alpha\bigl(\nabla_{\boldsymbol{x}}\bar{p}_\alpha + g\bar{\rho}_\alpha\nabla_{\boldsymbol{x}}\bar{z}_\alpha\bigr)\\
&= \frac{G_{\alpha+1/2}}{2}(\boldsymbol{u}_{\alpha+1} + \boldsymbol{u}_\alpha) - \frac{G_{\alpha-1/2}}{2}(\boldsymbol{u}_\alpha + \boldsymbol{u}_{\alpha-1}) + \boldsymbol{K}_{\alpha+1/2} - \boldsymbol{K}_{\alpha-1/2},
\end{aligned}
\tag{5.11}
$$

where $\tilde{\phi}_{j,\alpha+1/2}$, $\tilde{f}_{j,\alpha+1/2}$, and $\tilde{a}_{j,3,\alpha+1/2}$ are given by (4.16), the mass transfer terms $G_{\alpha+1/2}$ for $\alpha = 1,\dots,M$ are given by (4.12) and (4.13), $\bar{p}_\alpha$, $\bar{z}_\alpha$ are given by (5.5) (but in original variables), and $\boldsymbol{K}_{\alpha+1/2}$ is specified by (5.8).

### 5.4 Closure of the model

We close the system by assuming that the thickness of each layer $h_\alpha$ is a fixed fraction of the total height $h$, i.e., $h_\alpha = l_\alpha h$ for $\alpha = 1, \dots, M$, where $l_1, \dots, l_M$ are positive constants such as $l_1 + \dots + l_M = 1$. Furthermore, defining $m_\alpha := \bar{\rho}_\alpha h$, $\boldsymbol{q}_\alpha := \bar{\rho}_\alpha h \boldsymbol{u}_\alpha$, and $r_{j,\alpha} := \rho_j \phi_{j,\alpha} h$ for $\alpha = 1, \dots, M$ and $j = 0, \dots, N$, we can write the system (5.11) as follows:

$$
\begin{aligned}
&\partial_t m_\alpha + \nabla_{\boldsymbol{x}} \cdot \boldsymbol{q}_\alpha = \frac{1}{l_\alpha}(G_{\alpha+1/2} - G_{\alpha-1/2}), && \text{(5.12a)}\\
&\partial_t r_{j,\alpha} + \nabla_{\boldsymbol{x}} \cdot \left( \frac{r_{j,\alpha} \boldsymbol{q}_\alpha}{m_\alpha} \right) \\
&= \frac{1}{l_\alpha}(\tilde{\phi}_{j,\alpha+1/2} G_{\alpha+1/2} - \tilde{\phi}_{j,\alpha-1/2} G_{\alpha-1/2}) - \frac{\rho_j}{l_\alpha}(\tilde{f}_{j,\alpha+1/2} - \tilde{f}_{j,\alpha-1/2}) \\
&\quad + \frac{1}{l_\alpha}(\tilde{a}_{j,3,\alpha+1/2} - \tilde{a}_{j,3,\alpha-1/2}), \quad j = 1, \dots, N, && \text{(5.12b)}\\
&\partial_t \boldsymbol{q}_\alpha + \nabla_{\boldsymbol{x}} \cdot \left( \frac{\boldsymbol{q}_\alpha \otimes \boldsymbol{q}_\alpha}{m_\alpha} \right) + h\big(\nabla_{\boldsymbol{x}} \bar{p}_\alpha + g \bar{\rho}_\alpha \nabla_{\boldsymbol{x}} \bar{z}_\alpha\big) \\
&= \frac{1}{l_\alpha}(\tilde{\boldsymbol{u}}_{\alpha+1/2} G_{\alpha+1/2} - \tilde{\boldsymbol{u}}_{\alpha-1/2} G_{\alpha-1/2}) + \frac{1}{l_\alpha}(\boldsymbol{K}_{\alpha+1/2} - \boldsymbol{K}_{\alpha-1/2}), && \text{(5.12c)}
\end{aligned}
$$

where $\bar{p}_\alpha$, $\bar{z}_\alpha$, and the average $\tilde{\phi}_{j,\alpha+1/2}$ defined by (4.16) can be written as

$$
\bar{p}_\alpha = p_{\mathrm{S}} + g \sum_{\beta=\alpha+1}^{M} l_\beta m_\beta + \frac{g}{2} l_\alpha m_\alpha, \quad \bar{z}_\alpha = z_{\mathrm{B}} + h \sum_{\beta=1}^{\alpha-1} l_\beta + \frac{l_\alpha}{2} h, \quad \tilde{\phi}_{j,\alpha+1/2} = \frac{1}{2}\left( \frac{r_{j,\alpha+1}}{m_{\alpha+1}} + \frac{r_{j,\alpha}}{m_\alpha} \right), \quad (5.13)
$$

respectively, and for $\alpha = 1, \dots, M$ the average $\tilde{\boldsymbol{u}}_{\alpha+1/2}$ by

$$
\tilde{\boldsymbol{u}}_{\alpha+1/2} := \frac{1}{2}\left( \frac{\boldsymbol{q}_{\alpha+1}}{m_{\alpha+1}} + \frac{\boldsymbol{q}_\alpha}{m_\alpha} \right),
$$

Summing from $j = 0$ to $j = M$ the equations (5.12a) we get one equation for the total mass of the mixture, namely

$$
\partial_t \bar{m} + \nabla_{\boldsymbol{x}} \cdot \left( \sum_{\beta=1}^{M} l_\beta \boldsymbol{q}_\beta \right) = G_{M+1/2} - G_{1/2}, \quad (5.14)
$$

where $\bar{m} := \sum_{\beta=1}^{M} l_\beta m_\beta$ and $G_{M+1/2}$ and $G_{1/2}$ represent the mass transfer on the bottom and at the free surface, respectively.

Finally, we need to derive an explicit formula for the total interlayer mass fluxes. To this end and following [11], for a fixed layer $\alpha$ we consider the sums of the equations (5.12a) from layer 1 to layer $\alpha$ and from layer $\alpha + 1$ to layer $M$, obtaining the respective equations

$$
\sum_{\beta=1}^{\alpha} l_\beta (\partial_t m_\beta + \nabla_{\boldsymbol{x}} \cdot \boldsymbol{q}_\beta) = G_{\alpha+1/2} - G_{1/2}, \qquad \sum_{\gamma=\alpha+1}^{M} l_\gamma (\partial_t m_\gamma + \nabla_{\boldsymbol{x}} \cdot \boldsymbol{q}_\beta) = G_{M+1/2} - G_{\alpha+1/2}, \quad (5.15)
$$

Now, defining $L_\alpha := l_1 + \cdots + l_\alpha$ and using that $m_\alpha = \bar{\rho}_\alpha h$ can be written as

$$m_\alpha = \sum_{j=0}^{N} r_{j,\alpha} = \rho_0 h + \sum_{j=1}^{N} \frac{\rho_j - \rho_0}{\rho_j} r_{j,\alpha}, \tag{5.16}$$

we deduce from (5.15) the identities

$$L_\alpha \partial_t(\rho_0 h) + \sum_{\beta=1}^{\alpha}\sum_{j=1}^{N} l_\beta \partial_t r_{j,\beta} \frac{\rho_j - \rho_0}{\rho_j} + \sum_{\beta=1}^{\alpha} l_\beta \nabla_{\boldsymbol{x}} \cdot \boldsymbol{q}_\beta = G_{\alpha+1/2} - G_{1/2}, \tag{5.17}$$

$$(1 - L_\alpha)\partial_t(\rho_0 h) + \sum_{\gamma=\alpha+1}^{M}\sum_{j=1}^{N} l_\gamma \partial_t r_{j,\gamma} \frac{\rho_j - \rho_0}{\rho_j} + \sum_{\gamma=\alpha+1}^{M} l_\gamma \nabla_{\boldsymbol{x}} \cdot \boldsymbol{q}_\gamma = G_{M+1/2} - G_{\alpha+1/2}. \tag{5.18}$$

Subtracting (5.17) multiplied by $(1 - L_\alpha)$ from (5.18) multiplied by $L_\alpha$ we obtain an equation that does not depend on $\partial_t h$. Secondly, we use (5.12b) to neglect the dependence on $\partial_t r_{j,\beta}$. Then, using the following notation

$$\boldsymbol{R}_\beta := \boldsymbol{q}_\beta - \sum_{j=1}^{N} r_{j,\beta} \frac{\boldsymbol{q}_\beta}{m_\beta} \frac{\rho_j - \rho_0}{\rho_j}, \quad \bar{\boldsymbol{R}} := \sum_{\beta=1}^{M} l_\beta \boldsymbol{R}_\beta,$$

we deduce

$$\begin{aligned}
&G_{\alpha+1/2}\left(1 - \sum_{j=1}^{N} \frac{\rho_j - \rho_0}{\rho_j}\tilde{\phi}_{j,\alpha+1/2}\right) - (1 - L_\alpha)G_{1/2}\left(1 - \sum_{j=1}^{N} \frac{\rho_j - \rho_0}{\rho_j}\tilde{\phi}_{j,1/2}\right) \\
&- L_\alpha G_{M+1/2}\left(1 - \sum_{j=1}^{N} \frac{\rho_j - \rho_0}{\rho_j}\tilde{\phi}_{j,M+1/2}\right) \\
&= \sum_{\beta=1}^{\alpha} l_\beta \nabla_{\boldsymbol{x}} \cdot (\boldsymbol{R}_\alpha - \bar{\boldsymbol{R}}) - \sum_{j=1}^{N} (\rho_j - \rho_0)\left(\tilde{f}_{j,\alpha+1/2} - \frac{\tilde{a}_{j,3,\alpha+1/2}}{\rho_j}\right) \\
&\quad + \sum_{j=1}^{N} (\rho_j - \rho_0)\left((1 - L_\alpha)\left(\tilde{f}_{j,1/2} - \frac{\tilde{a}_{j,3,1/2}}{\rho_j}\right) + L_\alpha\left(\tilde{f}_{j,M+1/2} - \frac{\tilde{a}_{j,3,M+1/2}}{\rho_j}\right)\right).
\end{aligned}$$

Taking into account the definition of $\tilde{\phi}_{j,\alpha+1/2}$ (5.13), we obtain

$$1 - \sum_{j=1}^{N} \frac{\rho_j - \rho_0}{\rho_j}\tilde{\phi}_{j,\alpha+1/2} = \frac{\rho_0}{\tilde{\rho}_{\alpha+1/2}}, \quad \text{where} \quad \tilde{\rho}_{\alpha+1/2} := \frac{2}{\dfrac{1}{\bar{\rho}_\alpha} + \dfrac{1}{\bar{\rho}_{\alpha+1}}}.$$

Finally, we deduce

$$G_{\alpha+1/2} = \frac{\tilde{\rho}_{\alpha+1/2}}{\rho_0} \sum_{\beta=1}^{\alpha} l_\beta \nabla_{\boldsymbol{x}} \cdot (\boldsymbol{R}_\beta - \bar{\boldsymbol{R}}) + G_{f-a,\alpha+1/2}, \tag{5.19}$$

where

$$G_{f-a,\alpha+1/2} := \frac{\tilde{\rho}_{\alpha+1/2}}{\rho_0}\left(-\sum_{j=1}^{N}(\rho_j-\rho_0)\left(\tilde{f}_{j,\alpha+1/2}-\frac{\tilde{a}_{j,3,\alpha+1/2}}{\rho_j}\right)+(1-L_\alpha)C_{1/2}+L_\alpha C_{M+1/2}\right),$$

$$C_{l+1/2} := G_{l+1/2}\frac{\rho_0}{\tilde{\rho}_{l+1/2}}+\sum_{j=1}^{N}(\rho_j-\rho_0)\left(\tilde{f}_{j,l+1/2}-\frac{\tilde{a}_{j,3,l+1/2}}{\rho_j}\right) \quad \text{for } l=0 \text{ and } l=M.$$

## 6 Numerical scheme

We now devise a numerical method to discretize the final system, defined by equations (5.12b), (5.12c), and (5.14) with the explicit definition of mass transfer (5.19). We consider an implicit discretization of the terms $\boldsymbol{K}_{\alpha+1/2}-\boldsymbol{K}_{\alpha-1/2}$, corresponding to a vertical diffusion, so these terms will not be considered in what follows in this section. If we define $\boldsymbol{W}_\alpha := (m_\alpha, \boldsymbol{q}_\alpha, r_{1,\alpha}, \dots, r_{N,\alpha})^{\mathrm{T}}$, then the vector of unknowns of the system defined by (5.12b), (5.12c), and (5.14) is

$$\boldsymbol{W} = \boldsymbol{\mathcal{C}}\hat{\boldsymbol{W}} \tag{6.1}$$

where the matrix $\boldsymbol{\mathcal{C}} \in \mathbb{R}^{(M(N+2)+1)\times M(N+3)}$ is defined as follows. We define $\boldsymbol{e}_{i,N}$ to be the $i$-th $N$-dimensional unit vector ($i=1,\dots,N$) for general $N$, $\boldsymbol{I}_d$ to be the $d\times d$ identity matrix, $\boldsymbol{0}_d$ to be the zero vector of size $d$, and $\boldsymbol{0}$ (without index) to be a zero matrix of unspecified size. Then we define the $(N+2)\times(N+3)$ block $\boldsymbol{C} := \left[\boldsymbol{0}_{N+2}\ \boldsymbol{I}_{N+2}\right]$,

$$\boldsymbol{\mathcal{C}} = \begin{bmatrix} l_1\boldsymbol{e}_{1,N+3}^{\mathrm{T}} & l_2\boldsymbol{e}_{1,N+3}^{\mathrm{T}} & \cdots & l_M\boldsymbol{e}_{1,N+3}^{\mathrm{T}} \\ \boldsymbol{C} & \boldsymbol{0} & \cdots & \boldsymbol{0} \\ \boldsymbol{0} & \boldsymbol{C} & \ddots & \vdots \\ \vdots & \ddots & \ddots & \boldsymbol{0} \\ \boldsymbol{0} & \cdots & \boldsymbol{0} & \boldsymbol{C} \end{bmatrix},$$

and the $M(N+3)$ vector $\hat{\boldsymbol{W}} = (\boldsymbol{W}_\alpha)_{1\le\alpha\le M}$, where $\boldsymbol{W}_\alpha \in \mathbb{R}^{N+3}$.

Note that relation (6.1) allows us to connect the full system defined by (5.12a)–(5.12c) with the compact one defined by (5.12b), (5.12c) and (5.14). The compact system can be written as

$$\boldsymbol{\mathcal{C}}\big(\partial_t\hat{\boldsymbol{W}}+\nabla_{\boldsymbol{x}}\cdot\boldsymbol{F}(\hat{\boldsymbol{W}})+\boldsymbol{\mathcal{P}}(\hat{\boldsymbol{W}})\big) = \boldsymbol{\mathcal{C}}\big(\boldsymbol{\mathcal{G}}^{+}(\hat{\boldsymbol{W}})-\boldsymbol{\mathcal{G}}^{-}(\hat{\boldsymbol{W}})\big), \tag{6.2}$$

where analogously to $\hat{\boldsymbol{W}}$, each one of terms defining this system can be written by layers. That is, we define the vectors $\boldsymbol{\mathcal{P}} = (\boldsymbol{\mathcal{P}}_\alpha)_{1\le\alpha\le M}$ and $\boldsymbol{\mathcal{G}}^{\pm} = (\boldsymbol{\mathcal{G}}_\alpha^{\pm})_{1\le\alpha\le M}$, where $\boldsymbol{\mathcal{P}}_\alpha, \boldsymbol{\mathcal{G}}_\alpha^{\pm} \in \mathbb{R}^{N+3}$ and

$$\boldsymbol{\mathcal{G}}_\alpha^{\pm} = \frac{1}{l_\alpha}(\boldsymbol{U}_{\alpha\pm1/2}G_{\alpha\pm1/2}+\boldsymbol{\mathcal{G}}_{f-a,\alpha}^{\pm}),$$

where we define

$$\boldsymbol{\mathcal{P}}_\alpha := \left( \begin{array}{c} 0 \\ gm_\alpha \nabla_{\boldsymbol{x}}(z_{\mathrm{B}}+h) + gh^2 \left( \dfrac{l_\alpha}{2} + \displaystyle\sum_{\beta=\alpha+1}^{M} l_\beta \right) \nabla_{\boldsymbol{x}} \bar{\rho}_\alpha + gh \nabla_{\boldsymbol{x}} \left( h \displaystyle\sum_{\beta=\alpha+1}^{M} l_\beta (\bar{\rho}_\beta - \bar{\rho}_\alpha) \right) \\ \mathbf{0}_N \end{array} \right),$$

$$\boldsymbol{U}_{\alpha\pm 1/2}(\hat{\boldsymbol{W}}) := \begin{pmatrix} 1 \\ \tilde{\boldsymbol{u}}_{\alpha\pm1/2} \\ \tilde{\phi}_{1,\alpha\pm1/2} \\ \vdots \\ \tilde{\phi}_{N,\alpha\pm1/2} \end{pmatrix}, \quad \boldsymbol{\mathcal{G}}^{\pm}_{f-a,\alpha} := \begin{pmatrix} \mathbf{0}_3 \\ -\rho_1 \tilde{f}_{1,\alpha\pm1/2} + \tilde{a}_{1,3,\alpha\pm1/2} \\ \vdots \\ -\rho_N \tilde{f}_{j,\alpha\pm1/2} + \tilde{a}_{N,3,\alpha\pm1/2} \end{pmatrix}. \tag{6.3}$$

On the other hand, $\boldsymbol{F} \in \mathbb{R}^{M(N+3)\times 2}$ is a matrix that can be partitioned as

$$\boldsymbol{F} = \begin{bmatrix} \boldsymbol{F}_1 \\ \boldsymbol{F}_2 \\ \vdots \\ \boldsymbol{F}_M \end{bmatrix}, \quad \text{where} \quad \boldsymbol{F}_\alpha = \begin{bmatrix} \boldsymbol{q}_\alpha^{\mathrm{T}} \\ (1/m_\alpha)\boldsymbol{q}_\alpha \otimes \boldsymbol{q}_\alpha \\ (r_{1,\alpha}/m_\alpha)\boldsymbol{q}_\alpha^{\mathrm{T}} \\ \vdots \\ (r_{N,\alpha}/m_\alpha)\boldsymbol{q}_\alpha^{\mathrm{T}} \end{bmatrix} \in \mathbb{R}^{(N+3)\times 2}, \quad \alpha = 1,\dots,M.$$

Then, to propose a discretization of (6.2) in two horizontal space dimensions, we first study the properties of the system corresponding to one layer, that is, we fix $\alpha \in \{1,\dots,M\}$ and consider

$$\partial_t \boldsymbol{W}_\alpha + \nabla_{\boldsymbol{x}} \cdot \boldsymbol{F}_\alpha(\boldsymbol{W}_\alpha) + \boldsymbol{\mathcal{P}}_\alpha(\hat{\boldsymbol{W}}) = \boldsymbol{\mathcal{G}}^{+}_\alpha(\hat{\boldsymbol{W}}) - \boldsymbol{\mathcal{G}}^{-}_\alpha(\hat{\boldsymbol{W}}). \tag{6.4}$$

For a vector $\boldsymbol{\eta} = (\eta_1,\eta_2)^{\mathrm{T}} \in \mathbb{R}^2$ with $\|\boldsymbol{\eta}\|_2 = 1$ we define the matrices

$$\boldsymbol{T}_{\boldsymbol{\eta}} := \begin{bmatrix} 1 & 0 & 0 & \mathbf{0}_N^{\mathrm{T}} \\ 0 & \eta_1 & \eta_2 & \mathbf{0}_N^{\mathrm{T}} \\ 0 & -\eta_2 & \eta_1 & \mathbf{0}_N^{\mathrm{T}} \\ \mathbf{0}_N & \mathbf{0}_N & \mathbf{0}_N & \boldsymbol{I}_N \end{bmatrix} \in \mathbb{R}^{(N+3)\times(N+3)}, \quad \hat{\boldsymbol{T}}_{\boldsymbol{\eta}} := \boldsymbol{I}_M \otimes \boldsymbol{T}_{\boldsymbol{\eta}} \in \mathbb{R}^{M(N+3)\times M(N+3)}.$$

For $\boldsymbol{\eta}^\perp = (-\eta_2,\eta_1)^{\mathrm{T}}$ and $\boldsymbol{f}: \mathbb{R}^2 \to \mathbb{R}^2$ we have $\nabla_{\boldsymbol{x}} \cdot \boldsymbol{f} = \partial_{\boldsymbol{\eta}}(\boldsymbol{f}\cdot\boldsymbol{\eta}) + \partial_{\boldsymbol{\eta}^\perp}(\boldsymbol{f}\cdot\boldsymbol{\eta}^\perp)$. Moreover, the quantities $\boldsymbol{U}_{\alpha\pm1/2}(\hat{\boldsymbol{W}})$ defined in (6.3) satisfy $\boldsymbol{T}_{\boldsymbol{\eta}}\boldsymbol{U}_{\alpha\pm1/2}(\hat{\boldsymbol{W}}) = \boldsymbol{U}_{\alpha\pm1/2}(\hat{\boldsymbol{T}}_{\boldsymbol{\eta}}\hat{\boldsymbol{W}})$, and $\boldsymbol{\mathcal{P}}_\alpha$ and $\boldsymbol{\mathcal{G}}^{\pm}_\alpha(\hat{\boldsymbol{W}})$ satisfy

$$\boldsymbol{T}_{\boldsymbol{\eta}}\boldsymbol{\mathcal{P}}_\alpha(\hat{\boldsymbol{W}}) = \boldsymbol{\mathcal{P}}_{\boldsymbol{\eta},\alpha}(\hat{\boldsymbol{W}}) + \boldsymbol{\mathcal{P}}_{\boldsymbol{\eta}^\perp,\alpha}(\hat{\boldsymbol{W}}) \tag{6.5}$$

with

$$\boldsymbol{\mathcal{P}}_{\boldsymbol{\eta},\alpha} = \left( gm_\alpha \partial_{\boldsymbol{\eta}}(z_{\mathrm{B}}+h) + gh^2 \left( \frac{l_\alpha}{2} + \sum_{\beta=\alpha+1}^{M} l_\beta \right) \partial_{\boldsymbol{\eta}} \bar{\rho}_\alpha + gh \partial_{\boldsymbol{\eta}} \left( h \sum_{\beta=\alpha+1}^{M} l_\beta (\bar{\rho}_\beta - \bar{\rho}_\alpha) \right) \right) \boldsymbol{e}_{2,N+3},$$

$$\boldsymbol{\mathcal{P}}_{\boldsymbol{\eta}^\perp,\alpha} = \left( gm_\alpha \partial_{\boldsymbol{\eta}^\perp}(z_{\mathrm{B}}+h) + gh^2 \left( \frac{l_\alpha}{2} + \sum_{\beta=\alpha+1}^{M} l_\beta \right) \partial_{\boldsymbol{\eta}^\perp} \bar{\rho}_\alpha + gh \partial_{\boldsymbol{\eta}^\perp} \left( h \sum_{\beta=\alpha+1}^{M} l_\beta (\bar{\rho}_\beta - \bar{\rho}_\alpha) \right) \right) \boldsymbol{e}_{3,N+3}.$$

and

$$\begin{aligned}\boldsymbol{T}_{\boldsymbol{\eta}}\boldsymbol{\mathcal{G}}^{\pm}_{\alpha}(\hat{\boldsymbol{W}}) &= \boldsymbol{U}_{\alpha\pm1/2}(\hat{\boldsymbol{T}}_{\boldsymbol{\eta}}\hat{\boldsymbol{W}})G_{\boldsymbol{\eta},\alpha\pm1/2} + \frac{1}{2}\boldsymbol{\mathcal{G}}^{\pm}_{f-a,\alpha}(\hat{\boldsymbol{T}}_{\boldsymbol{\eta}}\hat{\boldsymbol{W}})\partial_{\boldsymbol{\eta}}\big((\boldsymbol{x}-\bar{\boldsymbol{x}})^{\mathrm{T}}\boldsymbol{\eta}\big)\\ &\quad + \boldsymbol{U}_{\alpha\pm1/2}(\hat{\boldsymbol{T}}_{\boldsymbol{\eta}}\hat{\boldsymbol{W}})G_{\boldsymbol{\eta}^{\perp},\alpha\pm1/2} + \frac{1}{2}\boldsymbol{\mathcal{G}}^{\pm}_{f-a,\alpha}(\hat{\boldsymbol{T}}_{\boldsymbol{\eta}}\hat{\boldsymbol{W}})\partial_{\boldsymbol{\eta}^{\perp}}\big((\boldsymbol{x}-\bar{\boldsymbol{x}})^{\mathrm{T}}\boldsymbol{\eta}^{\perp}\big)\\ &=: \boldsymbol{\mathcal{G}}^{\pm}_{\boldsymbol{\eta},\alpha}(\hat{\boldsymbol{W}}) + \boldsymbol{\mathcal{G}}^{\pm}_{\boldsymbol{\eta}^{\perp},\alpha}(\hat{\boldsymbol{W}}),\end{aligned} \tag{6.6}$$

where $\boldsymbol{T}_{\boldsymbol{\eta}}\boldsymbol{\mathcal{G}}^{\pm}_{f-a,\alpha}(\hat{\boldsymbol{W}}) = \boldsymbol{\mathcal{G}}^{\pm}_{f-a,\alpha}(\hat{\boldsymbol{T}}_{\boldsymbol{\eta}}\hat{\boldsymbol{W}})$ and we have used that $G_{\alpha+1/2} = G_{\boldsymbol{\eta},\alpha+1/2} + G_{\boldsymbol{\eta}^{\perp},\alpha+1/2}$ with

$$\begin{aligned}G_{\boldsymbol{\eta},\alpha+1/2} &= \frac{\tilde{\rho}_{\alpha+1/2}}{\rho_0}\sum_{\beta=1}^{\alpha} l_{\beta}\big(\partial_{\boldsymbol{\eta}}(\boldsymbol{R}_{\alpha}-\bar{\boldsymbol{R}})\big)^{\mathrm{T}}\boldsymbol{\eta} + \frac{G_{f-a,\alpha+1/2}}{2}\partial_{\boldsymbol{\eta}}\big((\boldsymbol{x}-\bar{\boldsymbol{x}})^{\mathrm{T}}\boldsymbol{\eta}\big),\\ G_{\boldsymbol{\eta}^{\perp},\alpha+1/2} &= \frac{\tilde{\rho}_{\alpha+1/2}}{\rho_0}\sum_{\beta=1}^{\alpha} l_{\beta}\big(\partial_{\boldsymbol{\eta}^{\perp}}(\boldsymbol{R}_{\alpha}-\bar{\boldsymbol{R}})\big)^{\mathrm{T}}\boldsymbol{\eta}^{\perp} + \frac{G_{f-a,\alpha+1/2}}{2}\partial_{\boldsymbol{\eta}^{\perp}}\big((\boldsymbol{x}-\bar{\boldsymbol{x}})^{\mathrm{T}}\boldsymbol{\eta}^{\perp}\big).\end{aligned}$$

The system (6.4) can now be written as

$$\begin{aligned}&\partial_t\boldsymbol{W}_{\alpha} + \partial_{\boldsymbol{\eta}}\big(\boldsymbol{F}_{\alpha}(\boldsymbol{W}_{\alpha})\boldsymbol{\eta}\big) + \partial_{\boldsymbol{\eta}^{\perp}}\big(\boldsymbol{F}_{\alpha}(\boldsymbol{W}_{\alpha})\boldsymbol{\eta}^{\perp}\big) + \boldsymbol{T}_{\boldsymbol{\eta}}^{-1}\boldsymbol{\mathcal{P}}_{\boldsymbol{\eta},\alpha}(\hat{\boldsymbol{W}}) + \boldsymbol{T}_{\boldsymbol{\eta}}^{-1}\boldsymbol{\mathcal{P}}_{\boldsymbol{\eta}^{\perp},\alpha}(\hat{\boldsymbol{W}})\\ &= \boldsymbol{T}_{\boldsymbol{\eta}}^{-1}\boldsymbol{\mathcal{G}}^{+}_{\boldsymbol{\eta},\alpha}(\hat{\boldsymbol{W}}) + \boldsymbol{T}_{\boldsymbol{\eta}}^{-1}\boldsymbol{\mathcal{G}}^{+}_{\boldsymbol{\eta}^{\perp},\alpha}(\hat{\boldsymbol{W}}) - \boldsymbol{T}_{\boldsymbol{\eta}}^{-1}\boldsymbol{\mathcal{G}}^{-}_{\boldsymbol{\eta},\alpha}(\hat{\boldsymbol{W}}) - \boldsymbol{T}_{\boldsymbol{\eta}}^{-1}\boldsymbol{\mathcal{G}}^{-}_{\boldsymbol{\eta}^{\perp},\alpha}(\hat{\boldsymbol{W}}).\end{aligned}$$

Multiplying this system by $\boldsymbol{T}_{\boldsymbol{\eta}}$ and using that $\boldsymbol{F}_{\alpha}(\boldsymbol{W}_{\alpha})\boldsymbol{\eta} = \boldsymbol{T}_{\boldsymbol{\eta}}^{-1}[\boldsymbol{F}_{\alpha}]_1(\boldsymbol{T}_{\boldsymbol{\eta}}\boldsymbol{W}_{\alpha})$, where $[\boldsymbol{F}_{\alpha}]_1 = \boldsymbol{F}_{\alpha}\boldsymbol{e}_{1,2}$ is the first column of $[\boldsymbol{F}_{\alpha}]$, we obtain

$$\partial_t(\boldsymbol{T}_{\boldsymbol{\eta}}\boldsymbol{W}_{\alpha}) + \partial_{\boldsymbol{\eta}}[\boldsymbol{F}_{\alpha}]_1(\boldsymbol{T}_{\boldsymbol{\eta}}\boldsymbol{W}_{\alpha}) + \boldsymbol{\mathcal{P}}_{\boldsymbol{\eta},\alpha}(\hat{\boldsymbol{T}}_{\boldsymbol{\eta}}\hat{\boldsymbol{W}}) = \boldsymbol{\mathcal{G}}^{+}_{\boldsymbol{\eta},\alpha}(\hat{\boldsymbol{W}}) - \boldsymbol{\mathcal{G}}^{-}_{\boldsymbol{\eta},\alpha}(\hat{\boldsymbol{W}}) + S_{\boldsymbol{\eta}^{\perp}}, \tag{6.7}$$

where

$$\begin{aligned}S_{\boldsymbol{\eta}^{\perp}} = \boldsymbol{T}_{\boldsymbol{\eta}}\Bigg(&-\partial_{\boldsymbol{\eta}^{\perp}}\big(\boldsymbol{F}_{\alpha}(\boldsymbol{W}_{\alpha})\boldsymbol{\eta}^{\perp}\big) - \boldsymbol{T}_{\boldsymbol{\eta}}^{-1}\boldsymbol{\mathcal{P}}_{\boldsymbol{\eta}^{\perp},\alpha}(\hat{\boldsymbol{W}})\\ &+ \boldsymbol{T}_{\boldsymbol{\eta}}^{-1}\bigg(\boldsymbol{U}_{\alpha+1/2}(\hat{\boldsymbol{T}}_{\boldsymbol{\eta}}\hat{\boldsymbol{W}})G_{\boldsymbol{\eta}^{\perp},\alpha+1/2} + \frac{1}{2}\boldsymbol{\mathcal{G}}^{+}_{f-a,\alpha}(\hat{\boldsymbol{T}}_{\boldsymbol{\eta}}\hat{\boldsymbol{W}})\partial_{\boldsymbol{\eta}^{\perp}}\big((\boldsymbol{x}-\bar{\boldsymbol{x}})^{\mathrm{T}}\boldsymbol{\eta}^{\perp}\big)\bigg)\\ &- \boldsymbol{T}_{\boldsymbol{\eta}}^{-1}\bigg(\boldsymbol{U}_{\alpha-1/2}(\hat{\boldsymbol{T}}_{\boldsymbol{\eta}}\hat{\boldsymbol{W}})G_{\boldsymbol{\eta}^{\perp},\alpha-1/2} - \frac{1}{2}\boldsymbol{\mathcal{G}}^{-}_{f-a,\alpha}(\hat{\boldsymbol{T}}_{\boldsymbol{\eta}}\hat{\boldsymbol{W}})\partial_{\boldsymbol{\eta}^{\perp}}\big((\boldsymbol{x}-\bar{\boldsymbol{x}})^{\mathrm{T}}\boldsymbol{\eta}^{\perp})\big)\bigg)\Bigg).\end{aligned}$$

The numerical scheme is designed by defining a numerical approximation of the rotated system (6.7) at each edge of the control volumes grid, by neglecting tangential variations in each edge of the control volume, that is, neglecting the term $S_{\boldsymbol{\eta}^{\perp}}$, where $\boldsymbol{\eta}$ is the normal vector at each edge. Let us denote by $\{V_i\}_{i=1}^{N_c}$ control volumes that define a partition of the domain, by $E_{i,j}$ the interface between two adjacent control volume $V_i$ and $V_j$, being $\boldsymbol{\eta}_{i,j}$ the unitary normal vector from $V_i$ to $V_j$. For each control volume $V_i$ we define the set of neighboring control volumes by $K_i$ and by $|V_i|$ and $|E_{i,j}|$ the area and the length of each edge $E_{i,j}$ respectively. The center of mass of the control volume $V_i$ will be denoted by $\boldsymbol{x}_i$ and the center of the edge $E_{i,j}$ by $\boldsymbol{x}_{i,j}$.

The design of the numerical method is done by taking into account that the original system (6.2), multiplied by $\hat{\boldsymbol{T}}_{\boldsymbol{\eta}_{i,j}}$, is rewritten as (6.7). Then we denote by $\boldsymbol{W}_i^n$ the average values of the unknowns over the control volume $V_i$ at time $t^n$. We propose the following 2D finite volume method to approximate the system (6.2):

$$\boldsymbol{W}_i^{n+1} = \boldsymbol{W}_i^n - \frac{\Delta t}{|V_i|} \sum_{j \in K_i} |E_{i,j}| \boldsymbol{\mathcal{C}} \hat{\boldsymbol{T}}_{\boldsymbol{\eta}_{i,j}}^{-1} \big( \hat{\boldsymbol{\mathcal{F}}}_{i,j} + \hat{\boldsymbol{\mathcal{P}}}_{i,j} - \hat{\boldsymbol{\mathcal{G}}}_{i,j}^{+} + \hat{\boldsymbol{\mathcal{G}}}_{i,j}^{-} \big),$$

where

$$\hat{\boldsymbol{\mathcal{F}}}_{i,j} = (\boldsymbol{\mathcal{F}}_{i,j,\alpha})_{1 \leq \alpha \leq M}, \quad \hat{\boldsymbol{\mathcal{P}}}_{i,j} = (\boldsymbol{\mathcal{P}}_{i,j,\alpha})_{1 \leq \alpha \leq M}, \quad \hat{\boldsymbol{\mathcal{G}}}_{i,j}^{\pm} = (\boldsymbol{\mathcal{G}}_{i,j,\alpha}^{\pm})_{1 \leq \alpha \leq M}.$$

We define $\boldsymbol{\mathcal{F}}_{i,j,\alpha}$ for $\alpha = 1, \dots, M$ by an HLL-PVM-1U method [14] to define the first and second component. This approach relies on left and right bounds of the eigenvalues, $S_{\mathrm{L}}$ and $S_{\mathrm{R}}$, of the transport matrix of the full system. That implies to consider a HLL method of the full system and not a local independent method for each layer. For the other components we use that $\boldsymbol{\mathcal{F}}_{i,j,\alpha}$ is an approximation $[\boldsymbol{F}_\alpha]_1(\boldsymbol{T}_{\boldsymbol{\eta}} \boldsymbol{W}_\alpha)$ on edge $E_{i,j}$. Then, from the third component the flux components correspond to passive transport equations. Then we define for $k = 1, 2$

$$\begin{aligned}
[\mathcal{F}_{i,j,\alpha}]_k = \bigg[ & \frac{1}{2} \big( [\boldsymbol{F}_\alpha]_1 (T_{\eta_{i,j}} \boldsymbol{W}_{i,\alpha}) + [\boldsymbol{F}_\alpha]_1 (T_{\eta_{i,j}} \boldsymbol{W}_{j,\alpha}) \big) - \frac{1}{2} \Big( a_{0,i,j} \big( T_{\eta_{i,j}} (\boldsymbol{W}_{j,\alpha} - \boldsymbol{W}_{i,\alpha}) + \boldsymbol{b}_{i,j,\alpha} \big) \\
& + a_{1,i,j} \big( [\boldsymbol{F}_\alpha]_1 (T_{\eta_{i,j}} \boldsymbol{W}_{j,\alpha}) - [\boldsymbol{F}_\alpha]_1 (T_{\eta_{i,j}} \boldsymbol{W}_{i,\alpha}) + \mathcal{P}_{i,j,\alpha} \big) \Big) \bigg]_k
\end{aligned}$$

and for $k = 3, \dots, N+3$

$$[\mathcal{F}_{i,j,\alpha}]_k = [\mathcal{F}_{i,j,\alpha}]_1 \left( \frac{[T_{\eta_{i,j}} \boldsymbol{W}_{i,\alpha}]_k}{[T_{\eta_{i,j}} \boldsymbol{W}_{i,\alpha}]_1} \, \frac{1 + \operatorname{sgn}([\mathcal{F}_{i,j,\alpha}]_1)}{2} + \frac{[T_{\eta_{i,j}} \boldsymbol{W}_{j,\alpha}]_k}{[T_{\eta_{i,j}} \boldsymbol{W}_{j,\alpha}]_1} \, \frac{1 - \operatorname{sgn}([\mathcal{F}_{i,j,\alpha}]_1)}{2} \right).$$

The HLL-PVM-1U method is defined by the coefficients

$$a_{0,i,j} = \frac{S_{\mathrm{R},i,j}^n |S_{\mathrm{L},i,j}^n| - S_{\mathrm{L},i,j}^n |S_{\mathrm{R},i,j}^n|}{S_{\mathrm{R},i,j}^n - S_{\mathrm{L},i,j}^n}, \quad a_{1,i,j} = \frac{|S_{\mathrm{R},i,j}^n| - |S_{\mathrm{L},i,j}^n|}{S_{\mathrm{R},i,j}^n - S_{\mathrm{L},i,j}^n}.$$

The characteristic velocities $S_{\mathrm{L},i,j}^n$ and $S_{\mathrm{R},i,j}^n$ are global approximations of the minimum and maximum wave speed of the rotated system (6.7) obtained by neglecting the tangential terms, that is, by setting $S_{\boldsymbol{\eta}_{i,j}}^{\perp} = 0$. In this case we obtain a 1D system evaluated at $\boldsymbol{T}_{\boldsymbol{\eta}_{i,j}} \hat{\boldsymbol{W}}$ with an extra passive scalar corresponding to the tangential velocity. This extra field does not modifies the maximum and minimum wave speeds of the 1D system. Then, taking into account the bound of the eigenvalues deduced in [11] for the 1D system we define $S_{\mathrm{L},i,j}$ and $S_{\mathrm{R},i,j}$ as follows:

$$S_{\mathrm{L},i,j} := \bar{u}_{i,j}^n - \Psi_{i,j}^n, \qquad S_{\mathrm{R},i,j} := \bar{u}_{i,j}^n + \Psi_{i,j}^n,$$

where

$$\begin{aligned}
\bar{u}_{i,j}^n &:= \frac{1}{M} \sum_{\beta=1}^{M} \frac{1}{2} \big( \boldsymbol{u}_{\beta,i}^n + \boldsymbol{u}_{\beta,j}^n \big)^{\mathrm{T}} \boldsymbol{\eta}_{i,j}, \\
\Psi_{i,j}^n &:= \frac{2M-1}{\sqrt{2M(2M-1)}} \left( 2 \sum_{\beta=1}^{M} (\bar{u}_{i,j}^n - u_{\beta,i,j}^n)^2 + \frac{g(h_i^n + h_j^n)}{2\rho_0} \left( \rho_0 + \frac{1}{M} \sum_{\beta=1}^{M} (2\beta - 1) \frac{\bar{\rho}_{\beta,i}^n + \bar{\rho}_{\beta,j}^n}{2} \right) \right)^{1/2}.
\end{aligned}$$

We define $\boldsymbol{\mathcal{P}}_{i,j,\alpha}$ to be zero for all components except for the second one. Specifically, we set

$$\begin{aligned}\boldsymbol{\mathcal{P}}_{i,j,\alpha} = \Biggl( & g\frac{m_{i,\alpha}^n + m_{j,\alpha}^n}{2}(z_{\mathrm{B},j} + h_j^n - z_{\mathrm{B},i} - h_i^n) + g\frac{(h_i^n)^2 + (h_j^n)^2}{2}\Biggl(\frac{l_\alpha}{2} + \sum_{\beta=\alpha+1}^{M} l_\beta\Biggr)(\bar{\rho}_{j,\alpha}^n - \bar{\rho}_{j,\alpha}^n) \\ & + g\frac{h_i^n + h_j^n}{2}\sum_{\beta=\alpha+1}^{M} l_\beta(m_{j,\beta}^n - m_{j,\alpha}^n + m_{i,\beta}^n - m_{i,\alpha}^n)\Biggr)\boldsymbol{e}_{2,N+3}, \end{aligned} \tag{6.8}$$

$$\boldsymbol{\mathcal{G}}_{i,j,\alpha}^{\pm} = \boldsymbol{U}_{i,j,\alpha\pm1/2}G_{i,j,\alpha\pm1/2} + \frac{1}{2}\boldsymbol{\mathcal{G}}_{i,f-a,\alpha}^{\pm}(\boldsymbol{x}_{i,j} - \boldsymbol{x}_i)^{\mathrm{T}}\boldsymbol{\eta}_{i,j}, \tag{6.9}$$

where

$$\begin{aligned}\boldsymbol{U}_{i,j,\alpha\pm1/2} &= \frac{1}{4}\bigl(\boldsymbol{U}(\boldsymbol{T}_{\boldsymbol{\eta}_{i,j}}\boldsymbol{W}_{i,\alpha}) + \boldsymbol{U}(\boldsymbol{T}_{\boldsymbol{\eta}_{i,j}}\boldsymbol{W}_{j,\alpha}) + \boldsymbol{U}(\boldsymbol{T}_{\boldsymbol{\eta}_{i,j}}\boldsymbol{W}_{i,\alpha+1}) + \boldsymbol{U}(\boldsymbol{T}_{\boldsymbol{\eta}_{i,j}}\boldsymbol{W}_{j,\alpha+1})\bigr), \\ G_{i,j,\alpha+1/2} &= \frac{\tilde{\rho}_{i,j,\alpha+1/2}}{\rho_0}\sum_{\beta=1}^{\alpha} l_\beta\Bigl((\boldsymbol{R}_{j,\alpha} - \bar{\boldsymbol{R}}_j) - (\boldsymbol{R}_{i,\alpha} - \bar{\boldsymbol{R}}_i)\Bigr) + \frac{G_{i,f-a,\alpha+1/2}}{2}(\boldsymbol{x}_{i,j} - \boldsymbol{x}_i)^{\mathrm{T}}\boldsymbol{\eta}_{i,j}. \end{aligned} \tag{6.10}$$

By $\boldsymbol{\mathcal{G}}_{i,f-a,\alpha}^{\pm}$ and $G_{i,f-a,\alpha+1/2}$ we denote any second-order approximation of $\boldsymbol{\mathcal{G}}_{f-a,\alpha}^{\pm}$ and $G_{f-a,\alpha+1/2}$ at $\boldsymbol{x}_i$, respectively. Finally, in order to obtain a well-balanced finite volume solver we utilize the following definition of $\boldsymbol{b}_{i,j,\alpha}$,

$$\boldsymbol{b}_{i,j,\alpha} = \Biggl(\frac{\bar{\rho}_{i,\alpha}^n + \bar{\rho}_{j,\alpha}^n}{2}(z_{\mathrm{B},j} - z_{\mathrm{B},i})\Biggr)\boldsymbol{e}_{1,N+3}.$$

## 7 Numerical tests

In the following numerical simulations we use the global acceleration of gravity constants $g = 9.8\,\mathrm{m/s^2}$, $\phi_{\max} = 0.68$ (the (nominal) maximal total solids volume fraction), and employ the Richardson-Zaki hindered settling factor (2.8) with $n_{\mathrm{RZ}} = 4.7$. The viscosity and density of the pure fluid are $\mu_0 = 0.02416\,\mathrm{Pa\,s}$ and $\rho_0 = 1208\,\mathrm{kg/m^3}$, respectively, $\eta = \eta(\phi)$ is the concentration-dependent viscosity defined by $\eta(\phi) := \mu_0(1.0 - \phi/0.95)^{-\beta}$, $\beta = 2.5$. Other parameters in (2.4) are set $\sigma_0 = 0.22\,\mathrm{Pa}$, $\alpha = 5$ and the gel point $\phi_{\mathrm{c}} = 0.1$. In all tests the particles are assumed to have the same density $\rho_1 = \cdots = \rho_N = 2790\,\mathrm{kg/m^3}$.

### 7.1 Test 1: bidisperse sedimentation in a domain with a bump

In Test 1 we are interested in studying the behavior of a mixture with $N = 2$ different solid species dispersed in a viscous fluid with a viscosity $\mu_0$. In this first test we consider $\boldsymbol{T}^{\mathrm{E}} = \sigma_{\mathrm{e}} = 0$ (without viscous stress tensor and without compression). The solid particle diameters are $d_1 = 4.96 \times 10^{-4}\,\mathrm{m}$ and $d_2 = 3.25 \times 10^{-4}\,\mathrm{m}$ respectively. The discretization of the domain is given by $100 \times 100$ cells and $M = 10$ layers in the horizontal and vertical directions, respectively. The bottom elevation is given by

$$z_{\mathrm{B}}(x, y) = \exp\bigl(-40((x - 0.5)^2 + (y - 0.5)^2)\bigr)\,\mathrm{m} \tag{7.1}$$

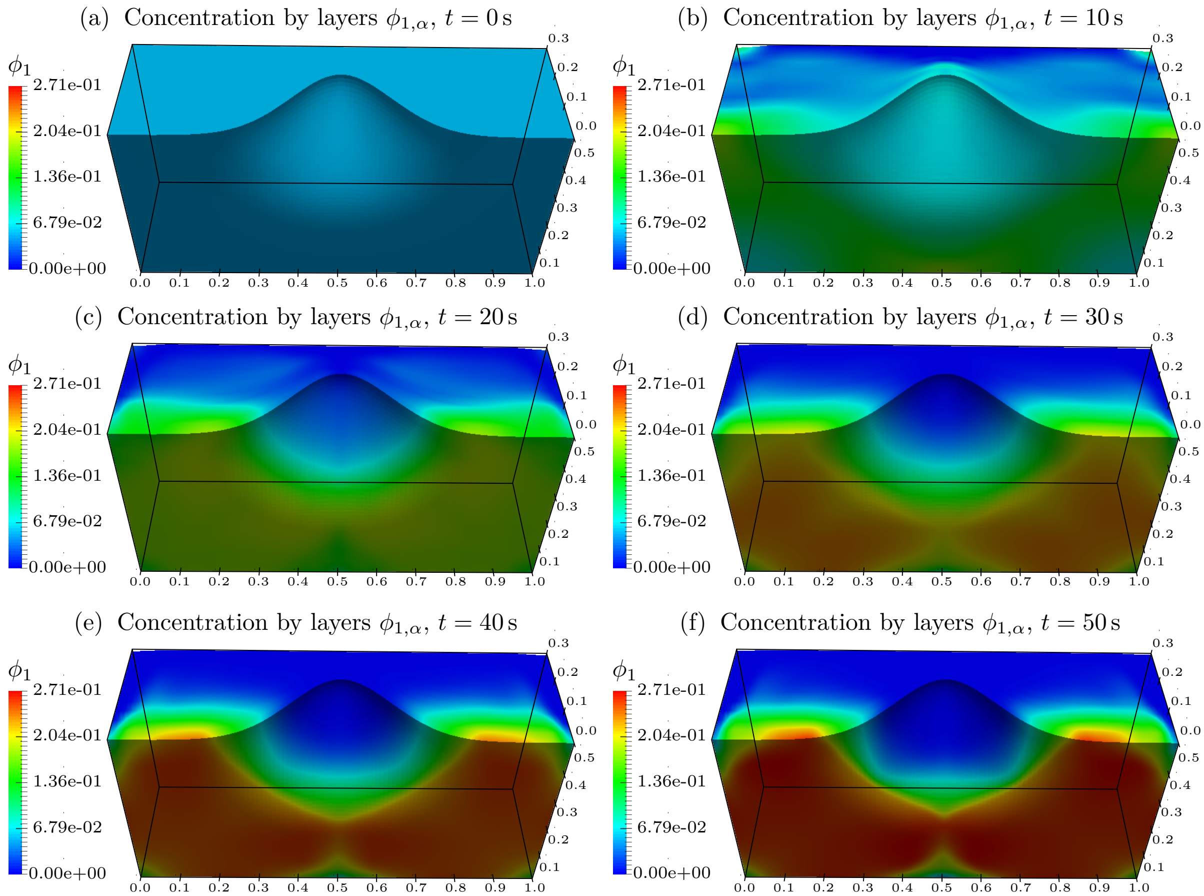


**Fig. 2** Test 1: Concentration of species 1 ($\phi_1$) by color in a domain with a bump.

for $(x, y) \in [0, 1] \times [0, 1]$. The initial condition for the concentrations and the horizontal velocities are given by

$$\phi_{1,\alpha}(0, x, y) = 0.05, \ \ \phi_{2,\alpha}(0, x, y) = 0.025, \ \ u_\alpha(0, x, y) = 0 \quad \text{for } \alpha = 1, \dots, M, \text{ and } (x, y) \in [0, 1] \times [0, 1].$$

The initial height is $h(0, x, y) = 0.3 - z_{\mathrm{B}}(x, y)$. Furthermore, as boundary condition we impose a closed basin.

In Figures 2, 3 and 4 we present the numerical results of the concentrations each species, $\phi_1$ and $\phi_2$, and the total concentration, respectively. This simulation is a three-dimensional version of [11, Test 2]. In Figure 2 high concentrations of species 1 can be observed since the bigger particles are deposited rapidly over the bottom around the bump. In Figure 3 we see how some fine particles remain in suspension close to the wall. At larger simulated times the smaller particles begin to settle and occupy zones where the concentration of species 1 is small, as can be seen in Figure 2 (f) and Figure 3 (f) at time $t = 50\,\mathrm{s}$. The joint behavior of all particles dispersed in the fluid is displayed in Figure 4. Here the global sedimentation

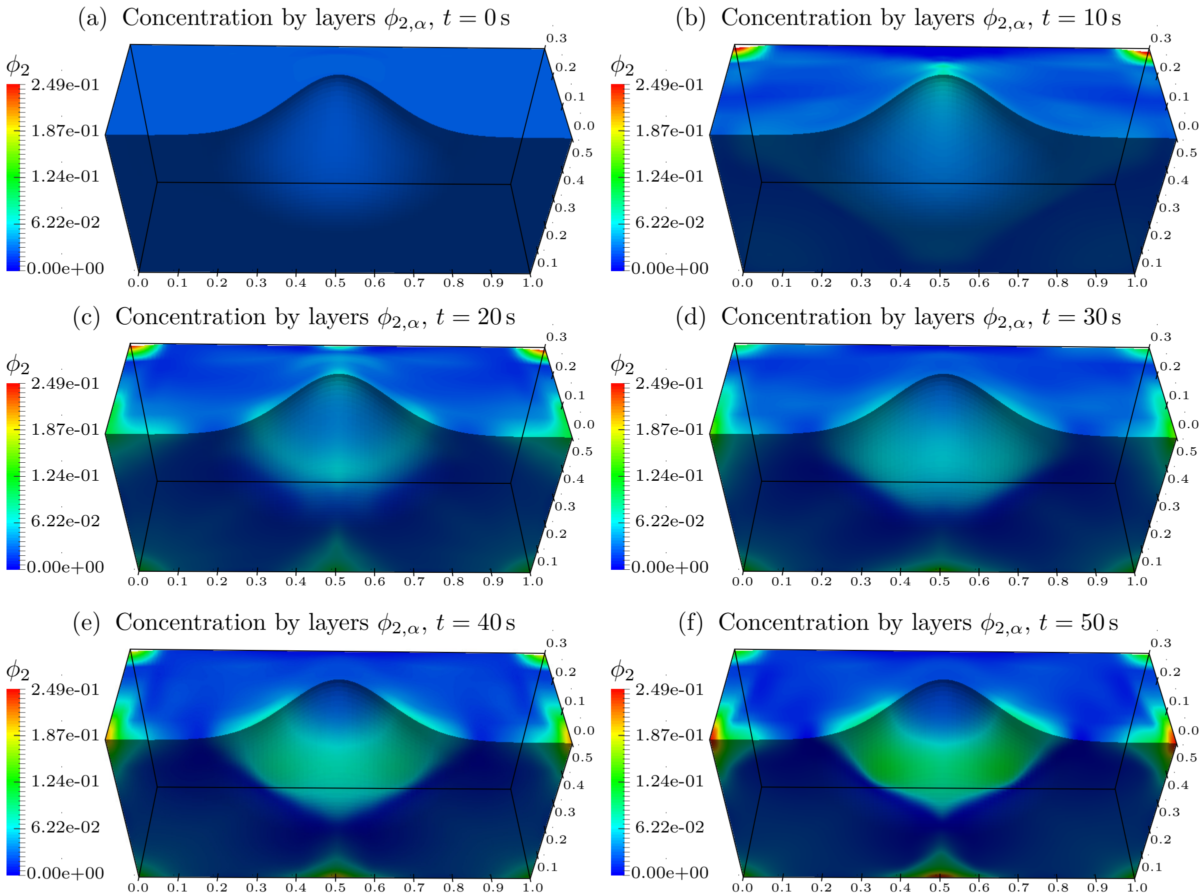


**Fig. 3** Test 1: Concentration of species 2 ($\phi_2$) by color in a domain with a bump.

process can be seen and we can see as the particles are deposited on the bottom around the bump but some fine particles (species 2) are kept in suspension at short times.

The velocity field of the mixture and its magnitude is presented in Figure 5 at different times. The movement of the mixture is a natural consequence of the movement of the particles. Some important recirculations can be seen around the bump. At larger times the velocity decreases and the particles settle more easily.

### 7.2 Test 2: cylindrical dam break

In this second numerical simulation we compare the behavior of the bidisperse sedimentation process with compression and mixture viscosity with the same mixture without compression and mixture viscosity in

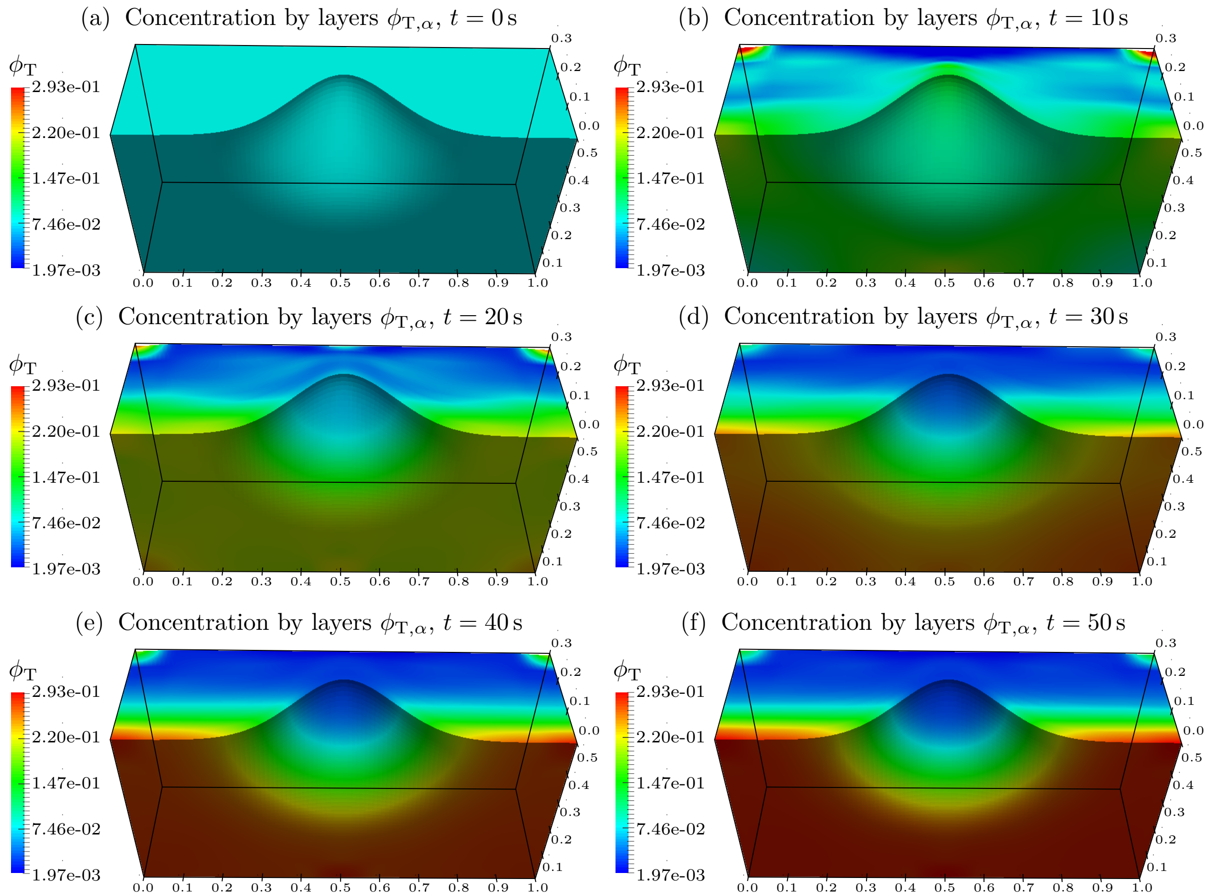


**Fig. 4** Test 1: Total concentration of solid particles, $\phi_{\mathrm{T}} = \phi_1 + \phi_2$ by color in a domain with a bump.

a paraboloid domain. To this we simulate a dam break problem over a paraboloid bottom given by

$$z_{\mathrm{B}}(x,y) = \begin{cases} 0.71((x-0.5)^2+(y-0.5)^2) & \text{for } (x-0.5)^2+(y-0.5)^2 \leq 0.21, \\ 0.15 & \text{otherwise,} \end{cases} \qquad (x,y) \in [0,1]\times[0,1].$$

The diameters of the solid particles are as in Test 1. Here we use a rectangular grid of $100 \times 100$ cells in the horizontal directions and $M = 10$ layers in the vertical direction. For all $\alpha = 1,\dots,M$ the initial condition is given by

$$\phi_{1,\alpha}(0,\boldsymbol{x}) = \begin{cases} 0.05 & \text{for } (x-0.2)^2+(y-0.5)^2 \leq 0.1, \\ 0 & \text{otherwise,} \end{cases} \qquad \boldsymbol{u}_\alpha(0,\boldsymbol{x}) = 0,$$

$$\phi_{2,\alpha}(0,\boldsymbol{x}) = \begin{cases} 0.025 & \text{for } (x-0.2)^2+(y-0.5)^2 \leq 0.1, \\ 0 & \text{otherwise,} \end{cases} \tag{7.2}$$

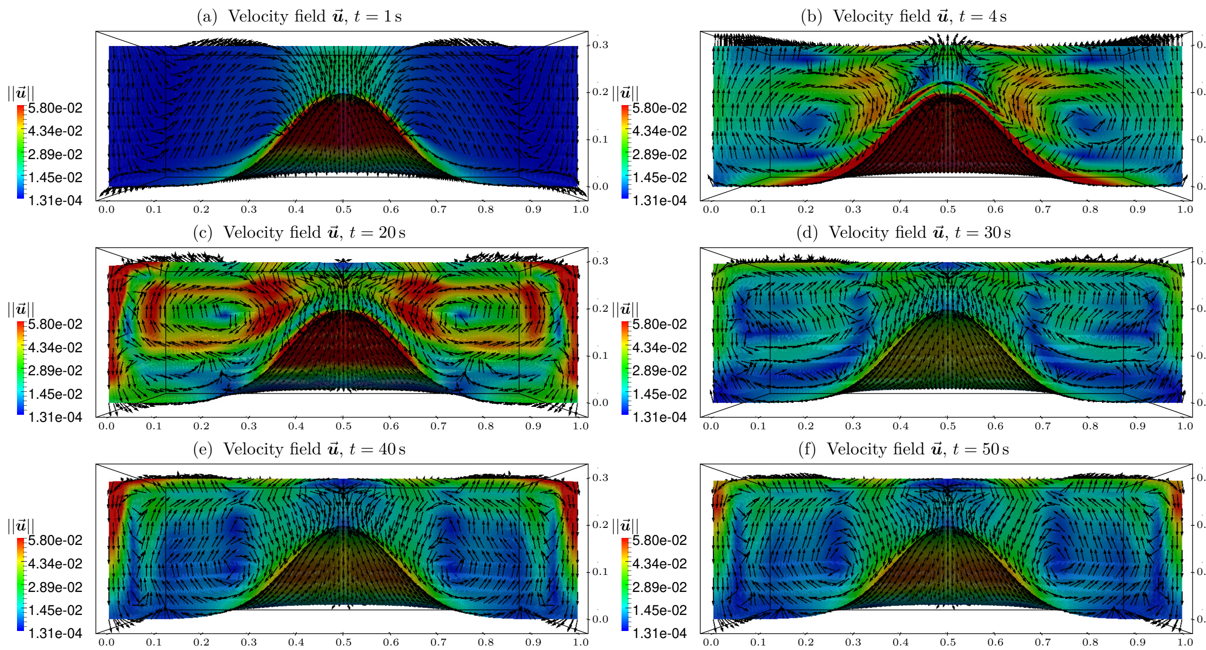


**Fig. 5** Test 1: Velocity field of the mixture over magnitude of the velocity.

and for the height $h(0, x, y) = 0.3 - z_{\mathrm{B}}(x, y)$. Figures 6, 7, 8 and 9 show the comparison between a simulation without compression and mixture viscosity Case 1 (left) and with them Case 2 (right) for bigger particles $\phi_1$ (species 1), fine particles $\phi_2$ (species 2), for the total concentration $\phi_T$ and for the velocity field of the mixture. The first that we can see is that in both cases the bigger particles go down faster than of the small particles, furthermore the small particles go to zones of the domain where the concentration of the bigger particles is small (Figure 6 (a), (c), (e) and Figure 7 (b), (d), (f), respectively). As we can see in Case 1 (left) in Figures 6, 7 and 8 (plots (a), (c) and (e) in each case), the movement of the solid particles in the mixture is oscillating for short times and from $t = 50\,$s the solid particles almost stop and from this time on the velocity field begins to be nearly symmetrical (see Figure 9 (a), (c), (e)). In Case 1 the solid particles move freely in the mixture. Insted, if we activate the compression and mixture viscosity terms (viscous stress) we can see from Figures 6, 7 and 8 (plots (b), (d) and (f) in each case) how the movement of the each solid species is slower than the Case 1, the reason is because for $\phi$ bigger than the gel point $\phi_{\mathrm{c}}$ the particles begin to compress and on the other hand when the concentration increases the viscosity of the mixture also increases, then the movement of the solid particles begins to be more dense than of the first case. In this Case 2 (right) the solid particles do not move oscillatorily as we can see in Figures 6, 7 and 8 (plots (b), (d) and (f) in each case). Finally, we comment that the velocity field is still not symmetrical at time $t = 50\,$s (see Figure 9 (b), (d), (f)). The mixture of Case 2 (right) moves with more difficulties that the mixture of Case 1.

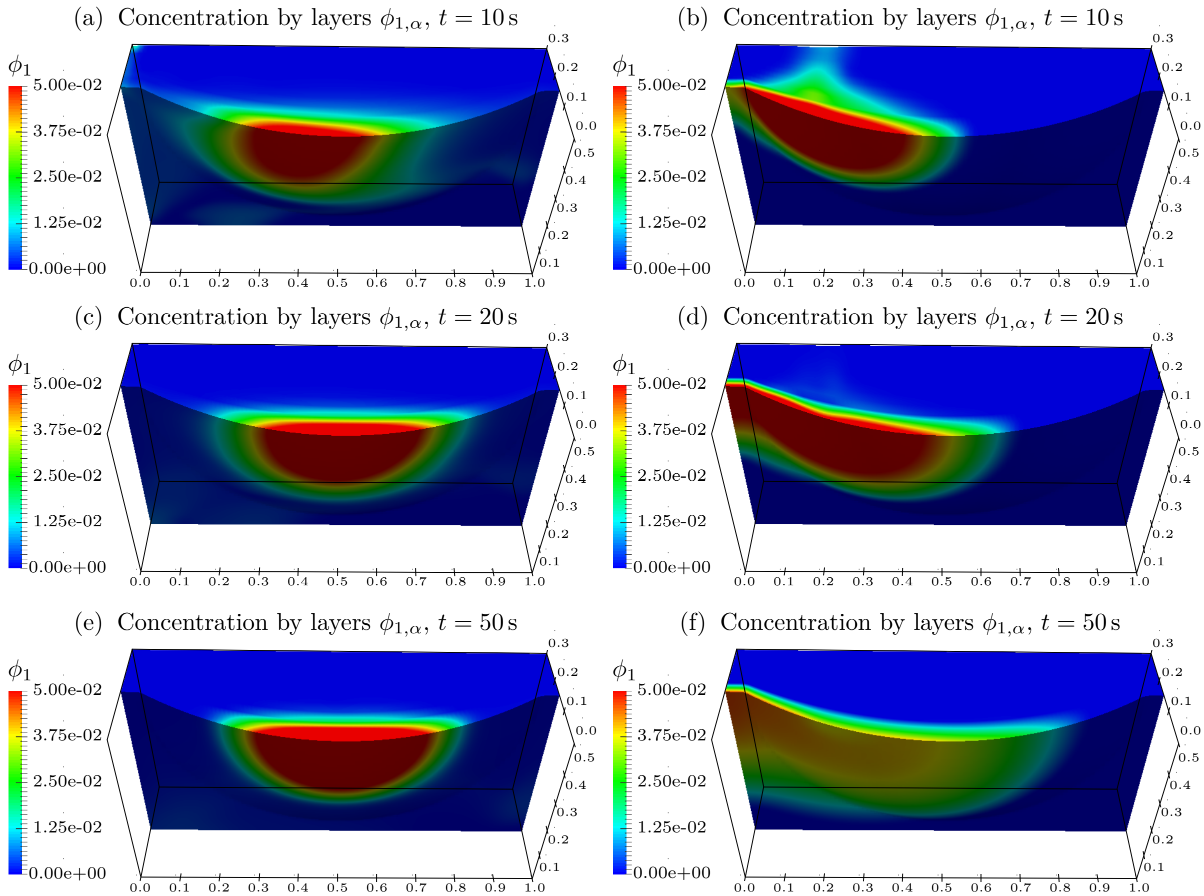


**Fig. 6** Test 2: Concentration of species 1 ($\phi_1$) by color in a 3D domain with compression and viscous stress tensor deactivated (left) versus concentration of species 1 with stress tensor and compression terms activated (right).

### 7.3 Test 3: bidisperse sedimentation process in real bathymetry for different gel point.

In the following numerical simulation we examine the behavior of the mixture when the gel point $\phi_{\mathrm{c}}$ is varied. To this we simulate a bi-bidisperse sedimentation process in a real configuration with compression and viscosity mixture terms activated. The bathymetry for this numerical simulation is given by

$$z_{\mathrm{B}}(x,y) = \begin{cases} 1.1 & 0 \le x < 0.4,\ 0 \le y \le 4, \\ 1.1 & 0.4 \le x \le 5.8-a,\ 0 \le y < a, \\ -\frac{1.1}{1.875-a}(y-a)+1.1 & 0.4 \le x \le 5.8-a,\ a \le y < \mathcal{L}_1, \\ -\frac{1.1}{5.3}(x-0.4)+1.1 & 0.4 \le x \le 5.8-a,\ \mathcal{L}_1 \le y \le \mathcal{L}_2, \\ -\frac{1.1}{(2.125-(4-a))}(y-(4-a))+1.1 & 0.4 \le x \le 5.8-a,\ \mathcal{L}_2 < y \le 4-a, \\ 1.1 & 0.4 \le x \le 5.8-a,\ 4-a < y \le 4, \\ z_{\mathrm{B}}(5.8-a,y) & 5.8-a < x \le 5.8,\ 0 \le y \le 4, \end{cases} \tag{7.3}$$

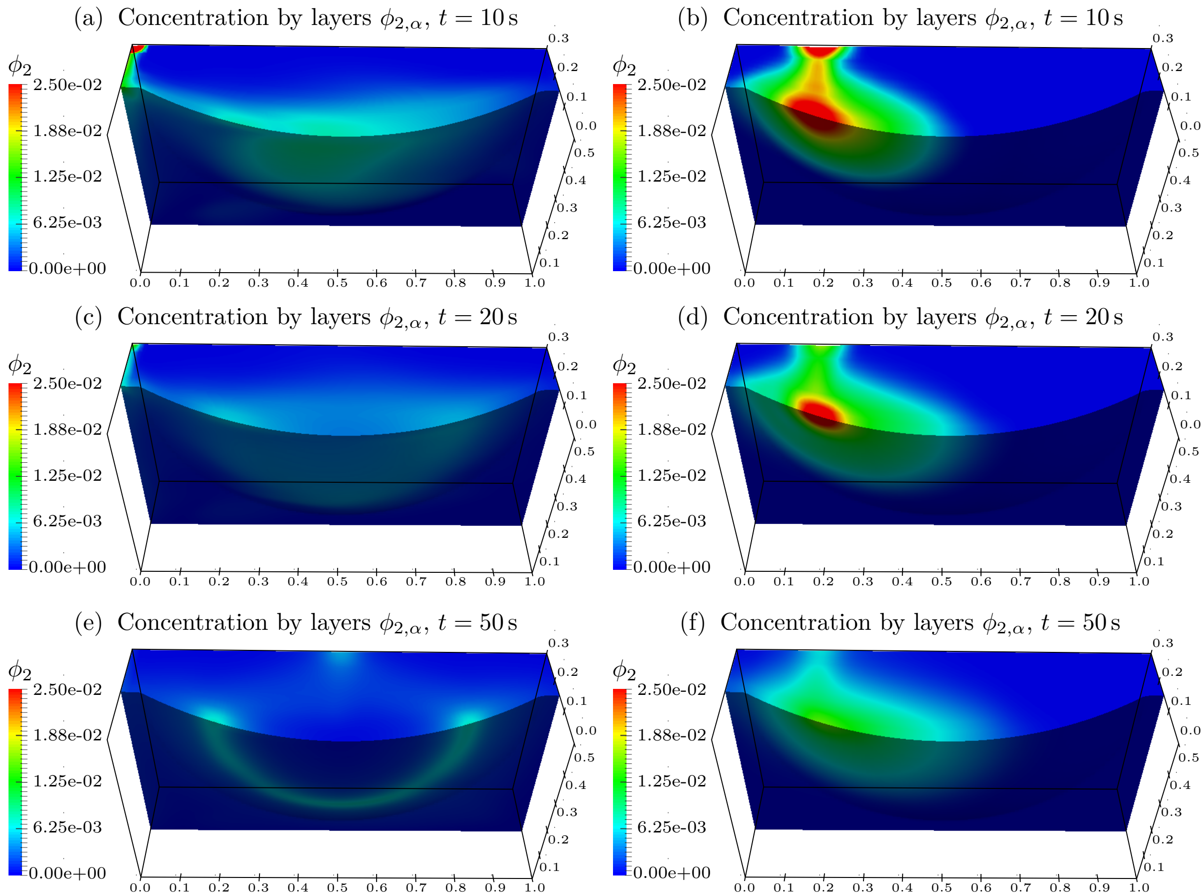


**Fig. 7** Test 2: Concentration of species 2 ($\phi_2$) by color in a 3D domain with compression and viscous stress tensor deactivated (left) versus concentration of species 2 with stress tensor and compression terms activated (right).

where the lines are given by $\mathcal{L}_1 : y = \frac{1.875-a}{5.3}(x-0.4)+a$, $\mathcal{L}_2 : y = \frac{2.125-(4-a)}{5.3}(x-0.4)+4-a$ and the parameter $a = 0.116$. The initial condition is the same that we have used in numerical Test 1,

$$\phi_{1,\alpha}(0,x,y) = 0.05, \;\; \phi_{2,\alpha}(0,x,y) = 0.025, \;\; u_\alpha(0,x,y) = 0 \text{ for } \alpha = 1,\dots,M, \text{ and } (x,y) \in [0,5.8]\times[0,4].$$

For the height $h(0,x,y) = 1.7 - z_{\mathrm{B}}(x,y)$ m. In this numerical simulation we only analyze the total concentration of the mixture Figure 11 and the concentration of the bigger particles in the mixture Figure 10 since it is for difficult to see differences in the behavior of the small particles dispersed in the mixture. In Figures 10 and 11 we can see the behavior of each species for different gel points, $\phi_{\mathrm{c}} = 0.08$ (left) and $\phi_{\mathrm{c}} = 0.15$ (right). Note that for small times when the compression is deactivated (before $\phi_{\mathrm{c}} = 0.08$) there is no difference in the concentrations. We will show only times when $\phi_{\mathrm{c}} \geq 0.08$. In this figure we can see that when the gel point is small, the particles begin to compress before they settle, and the movement of these particles is slow and they move with difficulties in the horizontal direction. This means that when we activate the gel point $\phi_{\mathrm{c}} = 0.08$ the particles essentially settle and with difficulties

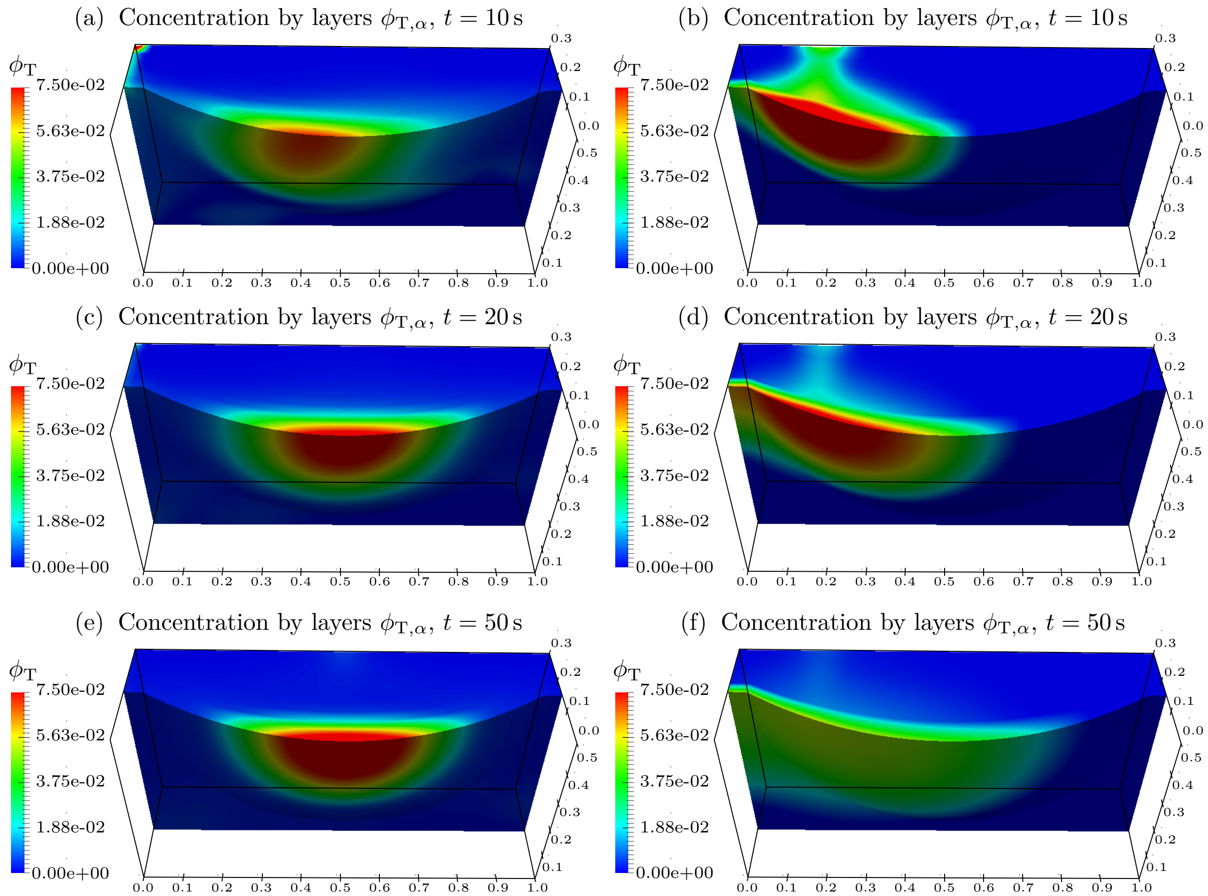


**Fig. 8** Test 2: Total concentration of solid particles $\phi_{\mathrm{T}} = \phi_1 + \phi_2$ by color in a 3D domain with compression and viscous stress tensor deactivated (left) versus total concentration of solid particles with stress tensor and compression terms activated (right).

move horizontally. They begin to compress anticipatedly (see Figure 10 (left), 11). On the other hand, when we active the gel point later $\phi_{\mathrm{c}} = 0.15$, first the particles settle faster than in the case before (see Figure 10 (b), (d) and (e)), and after the particles have settled they begin to compress and the movement of the particles begins to be more slow. We need to be careful with this comparison because if we see the equalities (2.4) keeping constant $\sigma_0$ we can observe two effects when $\phi_{\mathrm{c}}$ increases, first the compression starts later and the capacity of compression is smaller than when the $\phi_{\mathrm{c}}$ is small. Finally, Figure 12 shows the velocity field of the mixture only for gel point $\phi_{\mathrm{c}} = 0.15$ at some times, here we can see several recirculations at least one for each slope on the bottom.

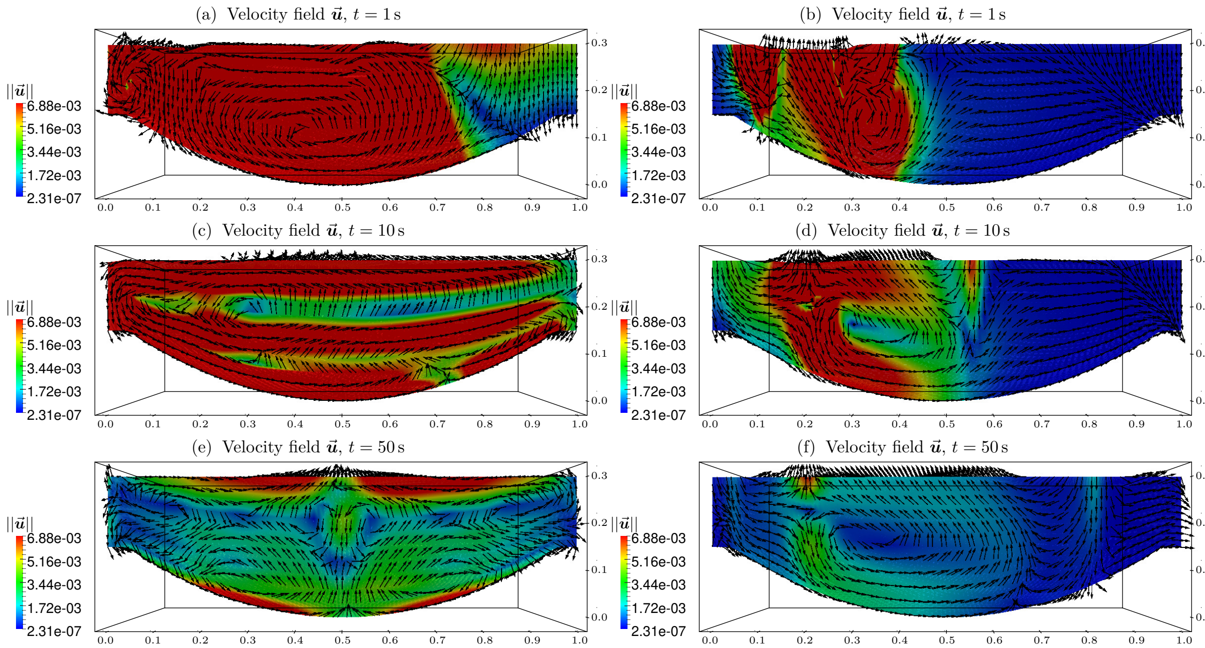

**Fig. 9** Test 2: Velocity field of mixture over her magnitud by color. Comparison between a a mixture with compression and viscous stress tensor deactivated (left) versus a mixture with stress tensor and compression terms activated (right).

### 7.4 Test 4: bidisperse sedimentation process in real bathymetry with different $\sigma_0$

The last numerical simulation shows a bidisperse sedimentation of the same mixture before (same diameters, densities, species), and initial and boundary conditions are as in Test 3. The bottom is given by 7.3. Here we keep constant the gel point $\phi_c = 0.1$ and study the behavior of the mixture when the parameter $\sigma_0$ in (2.4) is varied. This term represent the force or capacity of compression, it is clear from (2.4) that when $\sigma_0$ is increased, $\sigma_e$ increases as well (keeping constant the gel point). When the compression term is deactivated all species settle faster that when the compression term is activated and they move to the deepest zone. On the other hand, as we can see in Figures 13 and 14 with $\sigma_0 = 0.22$ (left) and $\sigma_0 = 0.88$ (right) if we active the compression term the particles begin to move with more difficulty to the deepest zone. In Figures 13 and 14 (b), (d), (f) for $\sigma_0 = 0.88$ we can see that the maximum of the concentration is smaller than of the maximum concentration for $\sigma_0 = 0.22$.

## 8 Conclusions

We have formulated a three-dimensional mathematical model to simulate polydisperse sedimentation that includes the compressibility of the sediment and the viscosity of the mixture. This model that can be used for simulations in industrial applications (clarification tanks, wastewater treatment) and geophysical flows such as sediment transport and polydisperse sedimentation in rivers. We have proposed a model that os vertically consistent with the classical 1D vertical model but with the property that

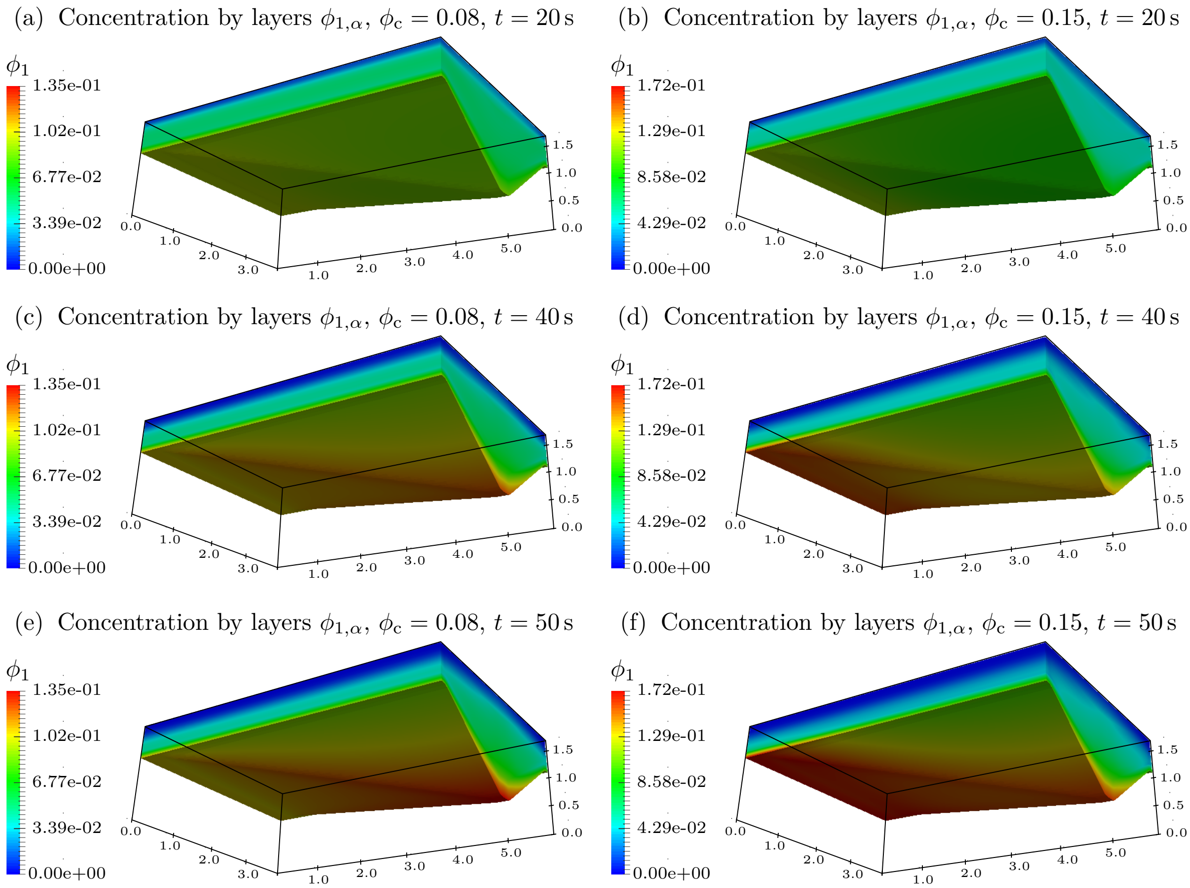


**Fig. 10** Test 4: Concentration of species 1 ($\phi_1$) by color with gel point $\phi_c = 0.08$ (left) versus concentration of species 1 with gel point $\phi_c = 0.15$ (right).

solid particles are transported in all directions. Naturally, under the assumption of shallow water, the compression term is essentially vertical. If we do not impose this assumption, the system (2.10)–(2.12) is much more complicated to solve since the compression term would be activated in all direction. This mathematical model allows on to know the concentration of each solid particle species dispersed in the fluid. For instance we get important information on areas where the concentration of the solid particles is below a tolerance index, in other words this model allow define zones where we can extract clean water. In this work the bottom or topography only varies with the space variable $z_B(x, y)$, but other important geophysical phenomena could also be modeled when the bottom vary respect to time $t$. Some future work is to design a mathematical model suitable to simulate erosion process, which means that the bottom can vary respect in time, and to describe sedimentation in an inclined channel.

(a) Concentration by layers $\phi_{\mathrm{T},\alpha}$, $\phi_{\mathrm{c}} = 0.08$, $t = 20\,\mathrm{s}$

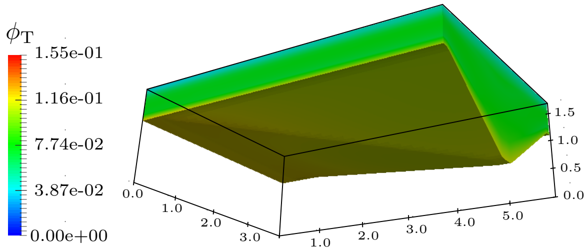


(b) Concentration by layers $\phi_{\mathrm{T},\alpha}$, $\phi_{\mathrm{c}} = 0.15$, $t = 20\,\mathrm{s}$

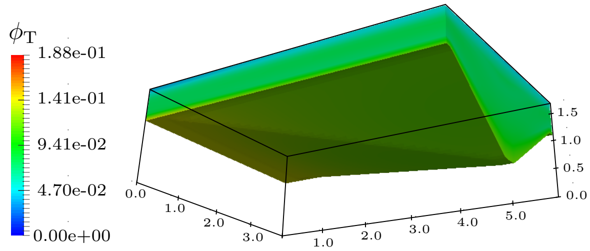


(c) Concentration by layers $\phi_{\mathrm{T},\alpha}$, $\phi_{\mathrm{c}} = 0.08$, $t = 40\,\mathrm{s}$

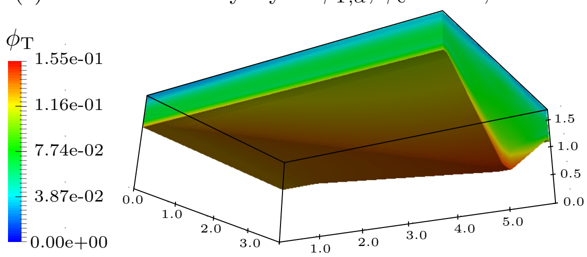


(d) Concentration by layers $\phi_{\mathrm{T},\alpha}$, $\phi_{\mathrm{c}} = 0.15$, $t = 40\,\mathrm{s}$

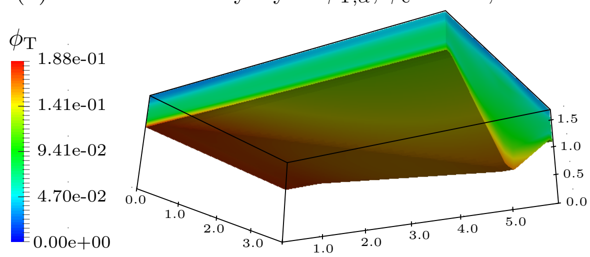


(e) Concentration by layers $\phi_{\mathrm{T},\alpha}$, $\phi_{\mathrm{c}} = 0.08$, $t = 50\,\mathrm{s}$

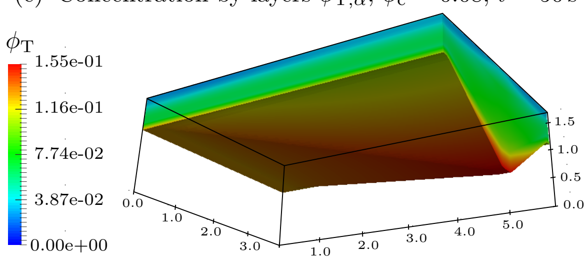


(f) Concentration by layers $\phi_{\mathrm{T},\alpha}$, $\phi_{\mathrm{c}} = 0.15$, $t = 50\,\mathrm{s}$

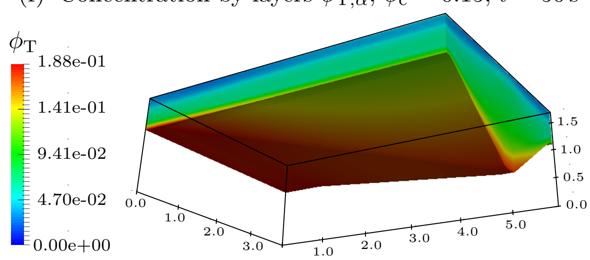


**Fig. 11** Test 4: Total concentration of solid species $\phi_{\mathrm{T}}$ with gel point $\phi_{\mathrm{c}} = 0.08$ (left) versus total concentration of solid species with gel point $\phi_{\mathrm{c}} = 0.15$ (right).

## Acknowledgments

RB is supported by Fondecyt project 1170473; CRHIAM, project CONICYT/FONDAP/15130015; and CONICYT/PIA/Concurso Apoyo a Centros Científicos y Tecnológicos de Excelencia con Financiamiento Basal AFB170001. EDFN is supported by the Spanish Government and FEDER through the Research project MTM 2015-70490-C2-2-R. VO is supported by CONICYT scholarship.

## References

1. Audusse, E.: A multilayer Saint-Venant model: derivation and numerical validation. Discrete Contin. Dyn. Syst. Ser. B **5**(2), 189–214 (2005). URL `https://doi.org/10.3934/dcdsb.2005.5.189`
2. Audusse, E., Bristeau, M., Perthame, B., Sainte-Marie, J.: A multilayer Saint-Venant system with mass exchanges for shallow water flows. derivation and numerical validation. ESAIM: Math. Model. Numer. Anal. **45**(1), 169–200 (2011). DOI 10.1051/m2an/2010036. URL `http://www-rocq.inria.fr/MACS/spip.php?article165`

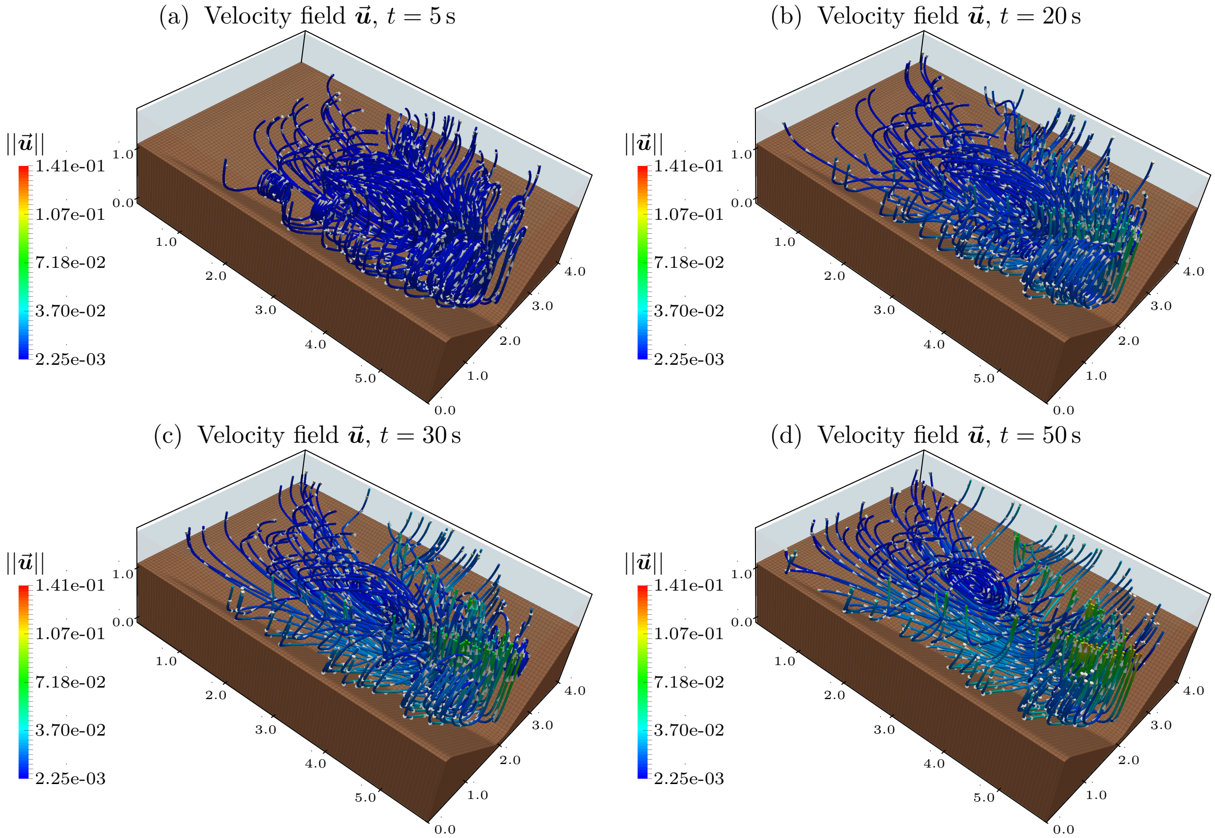


**Fig. 12** Test 4: Velocity field of the mixture with gel point $\phi_c = 0.15$.


3. Austin, L.G., Lee, C.H., Concha, F.: Hindered settling and classification partition curves. Minerals & Metallurgical Process. **9**(4), 161–168 (1992)
4. Berres, S., Bürger, R., Karlsen, K.H., Tory, E.M.: Strongly degenerate parabolic-hyperbolic systems modeling polydisperse sedimentation with compression. SIAM J. Appl. Math. **64**(1), 41–80 (2003). DOI 10.1137/S0036139902408163. URL `http://dx.doi.org/10.1137/S0036139902408163`
5. Bonnecaze, R.T., Huppert, H.E., Lister, J.R.: Patterns of sedimentation from polydispersed turbidity currents. Proc. Roy. Soc. Lond. A **452**, 2247–2261 (1996)
6. Boscarino, S., Bürger, R., Mulet, P., Russo, G., Villada, L.M.: Linearly implicit IMEX Runge-Kutta methods for a class of degenerate convection-diffusion problems. SIAM J. Sci. Comput. **37**(2), B305–B331 (2015). URL `https://doi.org/10.1137/140967544`
7. Boscarino, S., Bürger, R., Mulet, P., Russo, G., Villada, L.M.: On linearly implicit IMEX Runge-Kutta methods for degenerate convection-diffusion problems modeling polydisperse sedimentation. Bull. Braz. Math. Soc. (N. S.) **47**(1), 171–185 (2016). DOI 10.1007/s00574-016-0130-5. URL `https://doi.org/10.1007/s00574-016-0130-5`
8. Bürger, R., Diehl, S., Farås, S., Nopens, I., Torfs, E.: A consistent modelling methodology for secondary settling tanks: A reliable numerical method. Water Sci. Tech. **68**, 192–208 (2013). DOI 10.2166/wst.2013.239
9. Bürger, R., Diehl, S., Martí, M.C., Mulet, P., Nopens, I., Torfs, E., Vanrolleghem, P.A.: Numerical solution of a multiclass model for batch settling in water resource recovery facilities. Appl. Math. Model. **49**, 415–436 (2017). URL `https://doi.org/10.1016/j.apm.2017.05.014`
10. Bürger, R., Evje, S., Karlsen, K.H., Lie, K.A.: Numerical methods for the simulation of the settling of flocculated suspensions. Chem. Eng. J. **80**(1), 91–104 (2000). DOI https://doi.org/10.1016/S1383-5866(00)00080-0. URL `http:`

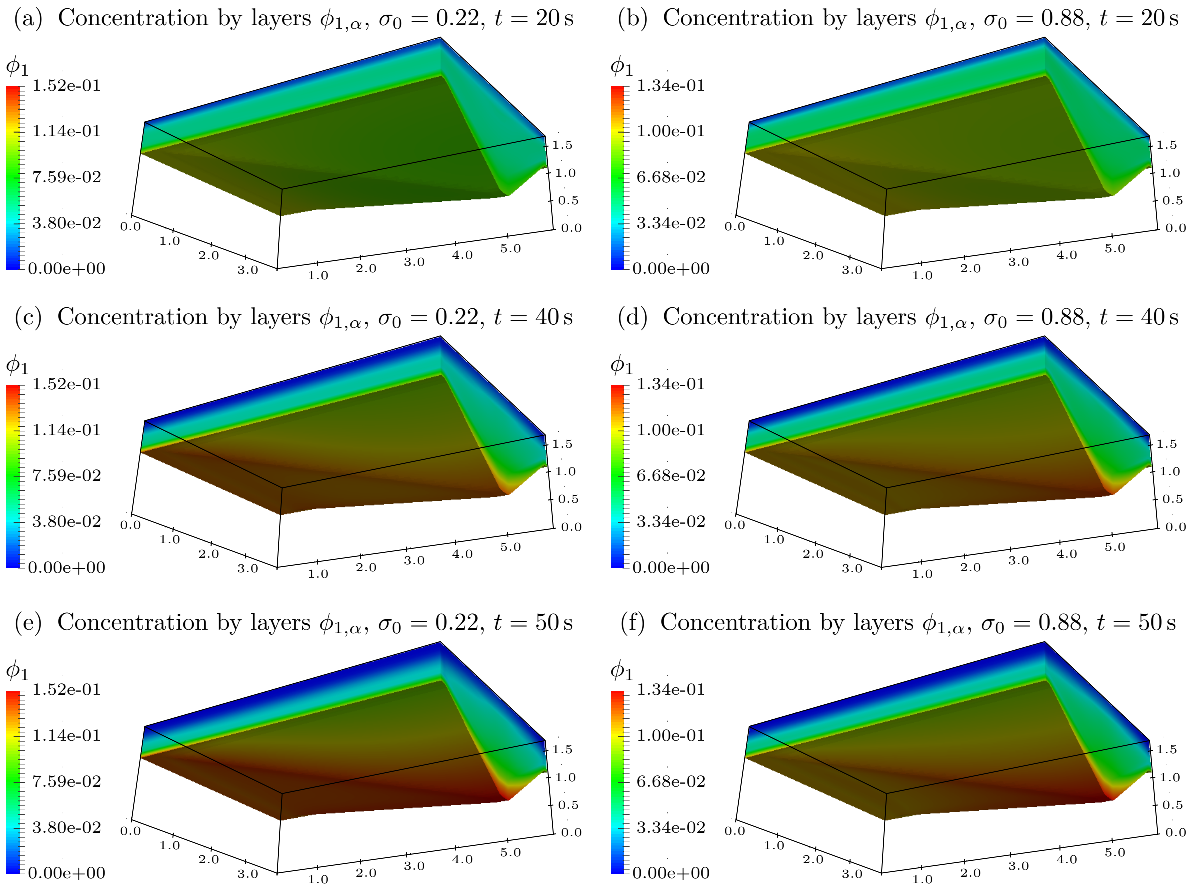


**Fig. 13** Test 4: Concentration of species 1 ($\phi_1$) by color with $\sigma_0 = 0.22$ (left) versus $\sigma_0 = 0.88$ (right) with a fixed gel point $\phi_c = 0.1$.

//www.sciencedirect.com/science/article/pii/S1383586600000800
11. Bürger, R., Fernández-Nieto, E.D., Osores, V.: A dynamic multilayer shallow water model for polydisperse sedimentation. ESAIM: Math. Model. Numer. Anal. **53**(5), 1391–1432 (2019). URL `https://doi.org/10.1051/m2an/2019032`
12. Bürger, R., Mulet, P., Villada, L.M.: Regularized nonlinear solvers for IMEX methods applied to diffusively corrected multispecies kinematic flow models. SIAM J. Sci. Comput. **35**(3), B751–B777 (2013). DOI 10.1137/120888533. URL `https://doi.org/10.1137/120888533`
13. Bürger, R., Wendland, W.L., Concha, F.: Model equations for gravitational sedimentation-consolidation processes. ZAMM Z. Angew. Math. Mech. **80**, 79–92 (2000)
14. Castro Díaz, M.J., Fernández-Nieto, E.: A class of computationally fast first order finite volume solvers: PVM methods. SIAM Journal on Scientific Computing **34**(4), A2173–A2196 (2012). DOI 10.1137/100795280. URL `http://epubs.siam.org/doi/abs/10.1137/100795280`
15. Diehl, S.: Shock-wave behaviour of sedimentation in wastewater treatment: A rich problem. In: K. Åström, L.E. Persson, S.D. Silvestrov (eds.) Analysis for Science, Engineering and Beyond, pp. 175–214. Springer Berlin Heidelberg, Berlin, Heidelberg (2012)
16. Fernández-Nieto, E.D., Koné, E.H., Chacón Rebollo, T.: A multilayer method for the hydrostatic Navier-Stokes equations: a particular weak solution. J. Sci. Comput. **60**(2), 408–437 (2014). URL `https://doi.org/10.1007/s10915-013-9802-0`

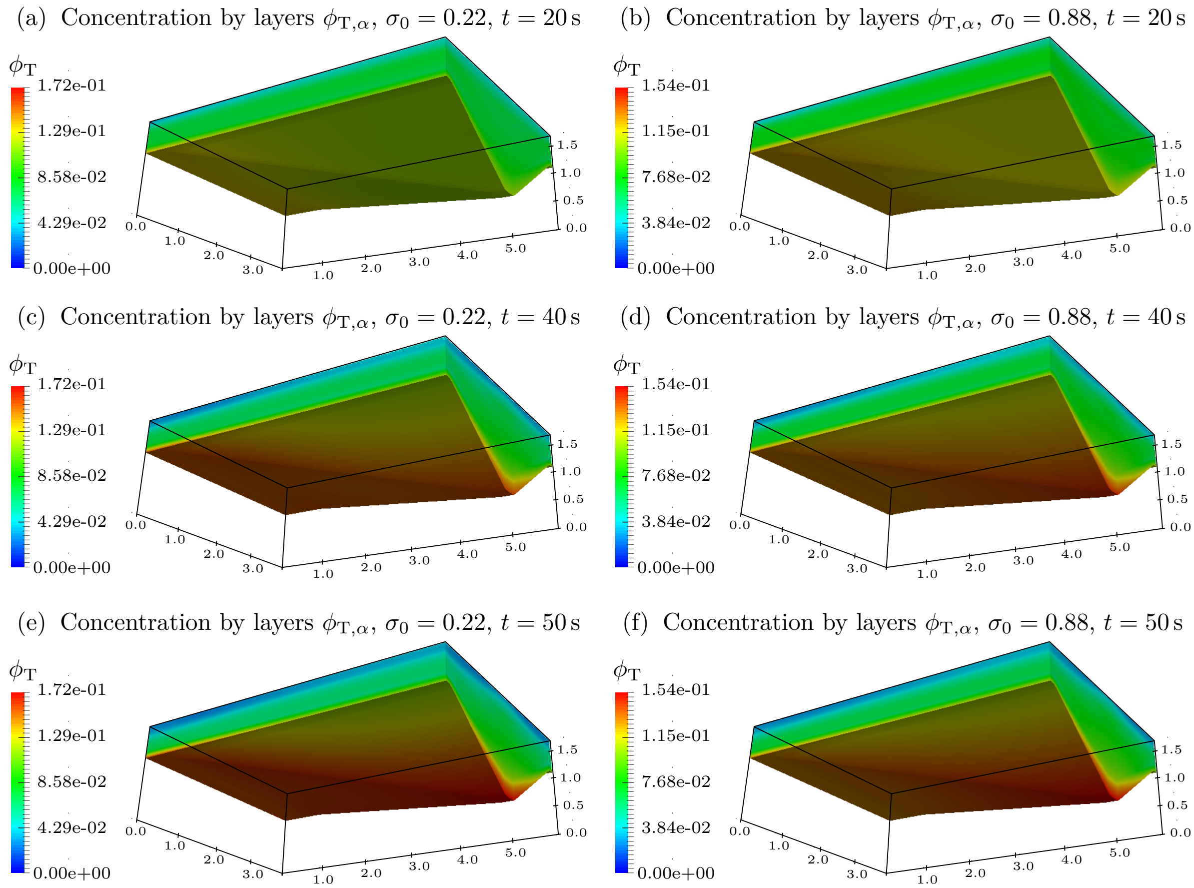


**Fig. 14** Test 4: Total concentration of solid species $\phi_\mathrm{T} = \phi_1 + \phi_2$ by color with $\sigma_0 = 0.22$ (left) versus $\sigma_0 = 0.88$ (right) with a fixed gel point $\phi_\mathrm{c} = 0.1$.

17. Fernández-Nieto, E.D., Koné, E.H., Morales de Luna, T., Bürger, R.: A multilayer shallow water system for polydisperse sedimentation. J. Comput. Phys. **238**, 281–314 (2013). DOI 10.1016/j.jcp.2012.12.008. URL `http://www.sciencedirect.com/science/article/pii/S0021999112007395`
18. Lockett, M.J., Bassoon, K.S.: Sedimentation of binary particle mixtures. Powder Technol. **24**, 1–7 (1979)
19. Masliyah, J.H.: Hindered settling in a multiple-species particle system. Chem. Engrg. Sci. **34**, 1166–1168 (1979)
20. Meiburg, E., Kneller, B.: Turbidity Currents and Their Deposits. Annual Review of Fluid Mechanics **42**(1), 135–156 (2010). DOI 10.1146/annurev-fluid-121108-145618. URL `http://dx.doi.org/10.1146/annurev-fluid-121108-145618`
21. Pérez, M., Font, R., Pastor, C.: A mathematical model to simulate batch sedimentation with compression behavior. Computers & Chemical Eng. **22**(11), 1531–1541 (1998). DOI https://doi.org/10.1016/S0098-1354(98)00246-4. URL `http://www.sciencedirect.com/science/article/pii/S0098135498002464`
22. Richardson, J.F., Zaki, W.N.: Sedimentation and fluidisation: Part I. Trans. Inst. Chem. Engrs. (London) **32**, 34–53 (1954)
23. Rushton, A., Ward, A.S., Holdich, R.G.: Solid-liquid filtration and sedimentation technology. 2nd ed., Wiley-VCH, Weinheim, Germany (2000)
24. Sainte-Marie, J.: Vertically averaged models for the free surface non-hydrostatic Euler system: derivation and kinetic interpretation. Math. Models Methods Appl. Sci. **21**(3), 459–490 (2011). URL `https://doi.org/10.1142/S0218202511005118`

# Centro de Investigación en Ingeniería Matemática (CI$^2$MA)

## PRE-PUBLICACIONES 2019



Para obtener copias de las Pre-Publicaciones, escribir o llamar a: Director, Centro de Investigación en Ingeniería Matemática, Universidad de Concepción, Casilla 160-C, Concepción, Chile, Tel.: 41-2661324, o bien, visitar la página web del centro: `http://www.ci2ma.udec.cl`

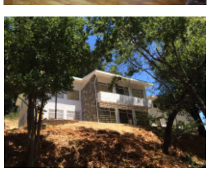

Centro de Investigación en
Ingeniería Matemática (CI$^2$MA)
**Universidad de Concepción**

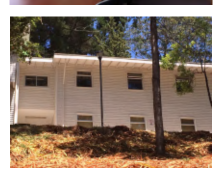

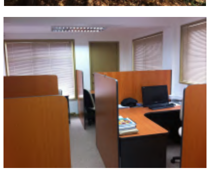

Casilla 160-C, Concepción, Chile
Tel.: 56-41-2661324/2661554/2661316
http://www.ci2ma.udec.cl